

## General Disclaimer

### One or more of the Following Statements may affect this Document

- This document has been reproduced from the best copy furnished by the organizational source. It is being released in the interest of making available as much information as possible.
- This document may contain data, which exceeds the sheet parameters. It was furnished in this condition by the organizational source and is the best copy available.
- This document may contain tone-on-tone or color graphs, charts and/or pictures, which have been reproduced in black and white.
- This document is paginated as submitted by the original source.
- Portions of this document are not fully legible due to the historical nature of some of the material. However, it is the best reproduction available from the original submission.

FINAL REPORT

OCEAN FOAM GENERATION  
AND MODELING

(NASA-CR-144922) OCEAN FOAM GENERATION AND  
MODELING Final Report (Radiometric  
Technology, Inc., Wakefield) 77 p HC \$5.00

N76-18770

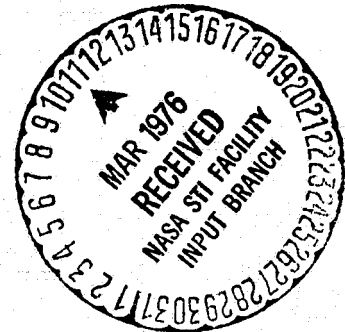
CSSL 08J

Unclas

G3/48 18435

by Ronald A. Porter  
and Kenneth P. Bechis

Contract No. NAS 1-13126



Prepared by

**RADIOMETRIC TECHNOLOGY, INC.**  
28C Vernon Street,  
Wakefield, Massachusetts 01880

Prepared for

National Aeronautics And Space Administration

## ABSTRACT

A study and laboratory investigation has been conducted to determine the physical and microwave properties of ocean foam. Special foam generators were designed and fabricated, using porous glass sheets, known as glass frits, as the principal element. The glass frit was sealed into a water-tight vertical box, a few centimeters from the bottom. Compressed air, applied to the lower chamber, created ocean foam from sea water lying on the frit. Foam heights of 30 cm were readily achieved, with relatively low air pressures.

Special photographic techniques and analytical procedures were employed to determine foam bubble size distributions. In addition, the percentage water content of ocean foam was determined with the aid of a particular sampling procedure.

A glass frit foam generator, with pore diameters in the range 70 - 100 micrometers, produced foam with bubble distributions very similar to those found on the surface of natural ocean foam patches.

## ACKNOWLEDGMENTS

The authors wish to thank Dr. James P. Hollinger, of the U.S. Naval Research Laboratory, for his suggestions relative to the use of glass frits for ocean foam generation.

In addition, the kind support of Mr. Bruce M. Kendall, of the NASA Langley Research Center is gratefully acknowledged.

Finally, the authors wish to thank Mr. Robert S. Howell, for his laboratory support, and Miss Marilyn R. Lawn for her valued assistance in the determination of foam bubble size distributions.

## TABLE OF CONTENTS

	<u>Page</u>
SECTION 1 - INTRODUCTION -----	1-1
SECTION 2 - METHODS OF FOAM GENERATION -----	2-1
2.1 Air Stone Method of Foam Generation -----	2-1
2.2 Air Diffuser Method of Foam Generation -----	2-1
2.3 Water Diffuser Method of Foam Generation -----	2-2
2.4 Water Jet Method of Foam Generation -----	2-3
2.5 Air-Water Jet Method of Foam Generation -----	2-3
2.6 Nylon Mesh Sheet Foam Generator -----	2-4
2.7 Glass Frit Method of Foam Generation -----	2-5
SECTION 3 - PHYSICAL AND MICROWAVE CHARACTERISTICS OF OCEAN FOAM -----	3-1
3.1 Results with First Foam Generator -----	3-1
3.2 Results with Second Foam Generator -----	3-19
3.3 Results with Third Foam Generator -----	3-28
3.4 In Situ Observations of Ocean Foam -----	3-29
SECTION 4 - TECHNIQUE FOR ROUTINE ANALYSIS OF OCEAN FOAM -----	4-1
4.1 Description of Method -----	4-1
4.2 Analysis of Sample Photographic Segment -----	4-3
SECTION 5 - DISCUSSION OF RESULTS -----	5-1
SECTION 6 - FULL-SCALE FOAM GENERATOR -----	6-1
SECTION 7 - CONCLUSIONS -----	7-1
SECTION 8 - RECOMMENDATIONS -----	8-1
SECTION 9 - REFERENCES -----	9-1
APPENDIX A - FOAM BUBBLE COUNTS OBTAINED WITH FIRST FOAM GENERATOR -----	A-1
APPENDIX B - FOAM BUBBLE COUNTS OBTAINED WITH SECOND FOAM GENERATOR -----	B-1

LIST OF ILLUSTRATIONS

<u>Figure No.</u>		<u>Page</u>
2-1	Layout Showing Foam Generator, Using Individual Glass Frit --	2-6
2-2	Foam Generator Experimental Setup -----	2-8
2-3	Foam Height as a Function of Applied Air Pressure (First Foam Generator) -----	2-10
3-1	Enlarged Photo of Sea Water Foam, 25-40 Micrometer Glass Frit	3-3
3-2	Sheet for Recording Foam Bubble Diameters, Counted in Selected Area on Enlarged Photo -----	3-4
3-3	Foam Bubble Count as a Function of Bubble Diameter and Depth Below Surface -----	3-5
3-4	Foam Bubble Count as a Function of Bubble Diameter and Depth Below Surface -----	3-6
3-5	Foam Bubble Count as a Function of Bubble Diameter and Depth Below Surface -----	3-7
3-6	Percentage of All Bubbles versus Bubble Diameter, for 25-40 Micrometer Frit -----	3-10
3-7	Percentage of Foam Bubbles with Diameters 0.5 mm (First Foam Generator) -----	3-12
3-8	Percentage of 0.6-1.0 mm Diameter Foam Bubbles (First Foam Generator) -----	3-13
3-9	Percentage of 1.1-1.5 mm Diameter Foam Bubbles (First Foam Generator) -----	3-14
3-10	Percentage Water Content of Ocean Foam as a Function of Total Foam Thickness -----	3-16
3-11	Enlarged Photo of Sea Water Foam, 10-20 Micrometer Glass Frit	3-21
3-12	Enlarged Photo of Sea Water Foam, 70-100 Micrometer Glass Frit	3-22

LIST OF ILLUSTRATIONS (Continued)

<u>Figure No.</u>		<u>Page</u>
3-13	Foam Bubble Count as a Function of Bubble Diameter and Depth Below Surface -----	3-23
3-14	Foam Bubble Count as a Function of Bubble Diameter and Depth Below Surface -----	3-24
3-15	Foam Bubble Count as a Function of Bubble Diameter and Depth Below Surface -----	3-25
3-16	Enlarged Photo of Natural Ocean Foam, with Meter Stick -----	3-30
4-1	Clear Plastic Template for Measurement of Foam Bubbles -----	4-2

LIST OF TABLES

<u>Table No.</u>		<u>Page</u>
2-1	Glass Frit Foam Generators Fabricated During Project -----	2-7
3-1	Electrical Characteristics of Ocean Foam at 1.4 GHz -----	3-18
3-2	Electrical Characteristics of Ocean Foam -----	3-27



## Section 1

### INTRODUCTION

The basic purpose of this study was to determine the physical and microwave properties of ocean foam. To this end, the contract required that a suitable technique be developed for the generation of representative ocean foam in the laboratory.

Following many attempts at generating foam, with a variety of different techniques, a particular method was discovered<sup>1</sup>. The method involves the use of a porous glass sheet, known as a glass frit, mounted a few centimeters above the bottom of a water-tight box. The frit is sealed into the box in a manner that will force the passage of compressed air, applied to the chamber below, through the frit. Air passing through the frit, and into a layer of sea water lying on it, produces foam of various heights, depending on the magnitude of the applied air pressure.

Five different glass frit foam generators were fabricated, using frits with pore diameters of 10-20, 25-40 and 70-100 micrometers. Four of the generators were used in comprehensive examinations and analyses of foam bubble size distributions. This was accomplished through the use of special photographic techniques, extensive bubble measurements and bubble counting procedures. In addition, the percentage water content of ocean foam was determined using the 70-100 micrometer foam generator.

Photographs were obtained of natural ocean foam, generated by the action of ocean swells at a rocky promontory in Marblehead, Massachusetts. Comparisons of the foam bubbles, recorded at the ocean, with those produced in the laboratory, showed that the 70-100 micrometer foam generator produced bubbles that were quite similar to those found in natural ocean foam. Accordingly, a full-size foam generator, utilizing glass frits with 70-100 micrometer pores was designed for fabrication and use by the NASA Langley Research Center. The dimensions of the foam area, to be generated by this unit, are 1.2 x 1.2 meters. The unit will be used in a roof-top wave tank at NASA Langley, for radiometric measurements of the apparent temperatures of ocean foam and for further studies of its physical and microwave properties.

During the course of the laboratory investigations and ensuing studies, it was observed that 50% of the bubbles, produced in the 70-100 micrometer foam generator, were equal to or greater than 0.6 mm in diameter. In the top 4 cm, the mean diameter ranged from 1.55 to 1.70 mm. The maximum diameter of foam bubbles, observed in the study, was 4 mm.

The water content of the top 4 cm of foam, produced by the 70-100 micrometer foam generator, was found to be 28%, for total foam depths in excess of 7 cm. Based on this information, it was possible to determine the electrical characteristics of ocean foam by considering it to be a porous medium. The dielectric permittivities were calculated at three microwave frequencies, together with electrical skin depths and attenuations. The skin depth of ocean foam is 2.0 cm at 1.43 GHz, 1.5 cm at 2.65 GHz and 0.32 cm at 10.69 GHz.

As far as is known, comprehensive data, of the type generated in this study, has not been available from any other research conducted prior to the publication of this report. There has been a strong need for this type of information during the past few years. It is felt that its availability will be of considerable value in the development of accurate microwave techniques for remote sensing of rough ocean surfaces.

## Section 2

### METHODS OF FOAM GENERATION

Several methods were investigated for ocean foam generation in the laboratory. These included the use of a special air stone; an air diffuser, consisting of a perforated plastic pipe with a nylon mesh covering; a water diffuser; a water jet; special air-water nozzles; a flat sheet of nylon mesh; and glass frits. These methods will be discussed individually, in chronological order, in the following paragraphs.

#### 2.1 AIR STONE METHOD OF FOAM GENERATION

A cylindrically-shaped air stone, 6.4 cm in outside diameter and 61 cm long, with pore diameters of 40 micrometers, was the first item to be investigated for generating ocean foam in the laboratory. This element was placed in a glass aquarium of 75 litre capacity. Approximately 25 litres of fresh sea water were poured into the aquarium. A small air compressor, with a maximum air pressure capability of 7 Kg/cm<sup>2</sup> (100 psi) and air flow rate of 3 litres/sec, (6.3 ft<sup>3</sup>/min) was connected to the air stone. The sea water had a salinity of 29 parts per thousand, a temperature of 21°C and conductivity of 40,000 micromhos/cm.

Various air pressures and flow rates were used in attempts to generate foam, with little success. A considerable amount of turbulence was created above the air stone, by air escaping through the air stone pores; this propelled the small amount of foam, produced by the air stone, to the sides of the aquarium. The maximum thickness of foam, generated with this method, was approximately 0.5 cm, with only about one-third of the water surface covered by foam. It was clear, therefore, that this method would not produce a sufficient volume of foam for a proper study of its physical and microwave characteristics.

#### 2.2 AIR DIFFUSER METHOD OF FOAM GENERATION

This method was a variant of the air stone technique described above. The diffuser consisted of a rigid, perforated polyethylene pipe with an inside diameter of 4 cm and length of 61 cm. A large number of perforations, of 3 mm diameter, were

drilled in the surface of the pipe, which was then covered with a double layer of nylon mesh with a mesh diameter of 40 micrometers. Another double layer of nylon, with a mesh diameter of 10 micrometers, was applied over this material. All joints were carefully sealed with epoxy cement.

The procedure observed in testing this foam generation technique was similar to that used with the air stone. The results were also quite similar in that only about a 0.5 cm thickness of foam was generated in the aquarium. The values of salinity, temperature and conductivity of the sea water, used in this experiment, were close to those cited in the discussion of the air stone method.

### 2.3 WATER DIFFUSER METHOD OF FOAM GENERATION

This method involved the use of an electrically-driven water pump, with the inlet and outlet hoses terminated in standard water diffusers. The water pump had a capacity of 3 litres/sec, and the hoses were of 4 cm inside diameter. Both water diffusers were immersed in a 30 cm depth of sea water in the aquarium. A small manually-operated valve was provided on the water pump to permit air to be drawn into the water during operation of the pump.

Although this method produced large numbers of small bubbles in the water, it generated less foam on its surface than the air stone and air diffuser methods. It was thought that this was due to the purifying action of the pump on the re-circulated water. Accordingly, another test was conducted on a boating pier in Ipswich, Massachusetts, to ensure a continuous supply of fresh sea water. The tests were performed at high tide; the water temperature varied between 18 and 22°C, the salinity ranged between 27 and 29 parts per thousand, and the conductivity varied from 39,000 to 40,000 micromhos/cm.

After the aquarium was half-filled with a 30-cm depth of water, a siphon was employed to maintain this water level. The outlet water diffuser was set on the bottom of the aquarium. Although slightly more foam was generated with this approach, the foam thickness was less than 0.5 cm. Accordingly, the water diffuser method was abandoned as a means of generating ocean foam.

## 2.4 WATER JET METHOD OF FOAM GENERATION

In this method, the water pump and air compressor forced an air-water mixture through a specially constructed flat nozzle, with inside dimensions of 6 cm by 0.8 mm. The water, emanating from the nozzle, was directed horizontally at a vertically-oriented fine-mesh wire screen, mounted in a baffle board placed near one end of the aquarium. The screen mesh diameter was approximately 0.5 mm. Provision was made to permit positioning of the screen, horizontally, over a distance of 0.5 to 10 cm from the tip of the nozzle.

The sea water salinity was 29 parts per thousand, the temperature was 21°C, and the conductivity was 40,000 micromhos/cm.

This method was the most successful of all those attempted so far; a thickness of 0.5 to 0.9 cm of foam was generated with this technique. However, this amount of foam was insufficient for purposes of this investigation.

## 2.5 AIR-WATER JET METHOD OF FOAM GENERATION

The encouraging results, obtained with the water jet method, indicated that a large-scale experiment would be justified, using an array of flat nozzles in a large water tank. A decision to conduct such an experiment was prompted, in part, by the need for a 1.2-meter-diameter foam patch for radiometric measurements in the NASA Langley Research Center roof-top wave tank.

A foam tank was constructed from 1.9-cm-thick exterior-type plywood. The tank was 1.2 x 1.7 x 0.4 meter high, with 0.4 x 0.3 meter glass windows, located in the centers of the long sides of the tank. The interior and exterior surfaces of the tank were coated with a marine sealer and all joints were filled with a waterproof caulking compound. A baffle board, running the full width and height of the tank and containing a 0.5-mm fine mesh screen in its central region, was installed near one end of the tank. Since the baffle board was held in place with C-clamps, it was possible to locate it at various positions, along the long dimension of the tank, without difficulty.

A 6-nozzle array was fabricated from 2.5-cm thin-wall copper tubing. The nozzles were formed by flattening the tubing for a distance of approximately 0.9 cm; the resultant inside dimensions of each nozzle were 1.55 x 0.08 cm. Nozzle spacing was 19 cm. Connections were provided for, both, air and water at the inlet of the array.

The above arrangement was tested in a depth of approximately 18 cm of fresh sea water. At first, only water was forced through the nozzles, with the water jet directed horizontally at the vertically-oriented baffle screen. Since this produced only a small amount of foam, an air-water mixture was injected by adding air from a large construction-type air compressor with an air pressure capacity of 8.5 Kg/cm<sup>2</sup> (120 psi) and an air flow rate of 38 litres/sec, (80 ft<sup>3</sup>/min).

The nozzles were pointed in various directions, in attempts to maximize the production of foam. First, they were pointed at the fine-mesh screen in the baffle board. Next, the baffle board was removed from the tank and the nozzles were immersed at various depths in the water. Since neither of these procedures resulted in more than a 0.5-cm thickness of foam, the nozzles were reversed, to point at the end wall of the tank. With full air and water pressures applied, the nozzles were placed at distances of 2 to 30 cm from the wall of the tank and at various depths in the water. The maximum thickness of foam that was generated was approximately 0.7 cm, over an area of 0.5 x 1.2 meters.

Due to the high air pressure, employed in this experiment, a considerable amount of spray was generated by the nozzle array. As in the case of the previously discussed foam generation techniques, this method was abandoned due to its inability to generate a sufficiently thick layer of foam.

## 2.6 NYLON MESH SHEET FOAM GENERATOR

This method of foam generation is based on a technique described by James P. Hollinger<sup>1</sup>. His method involved the use of fritted glass, with pore diameters of 30, 60 and 100 micrometers. The glass sheet was 30 cm square and 1 cm thick and was sealed in a square box, a few centimeters up from the bottom of the box. Under normal operation, a small amount of sea water was poured into the upper portion of

the box, to a depth of 3-4 cm. Air was applied to the bottom of the box and was evenly distributed over the bottom surface of the glass frit by small plastic foam particles. Very little air pressure was required to generate foam layers of several centimeters in height.

In view of Hollinger's success, it was decided to employ his method of foam generation for purposes of this study. However, since the delivery of the necessary glass frits would involve a period of three (3) months, it was decided to try out Hollinger's technique with the aid of a nylon mesh sheet in place of the glass frit. The mesh diameter in the nylon was 30 micrometers.

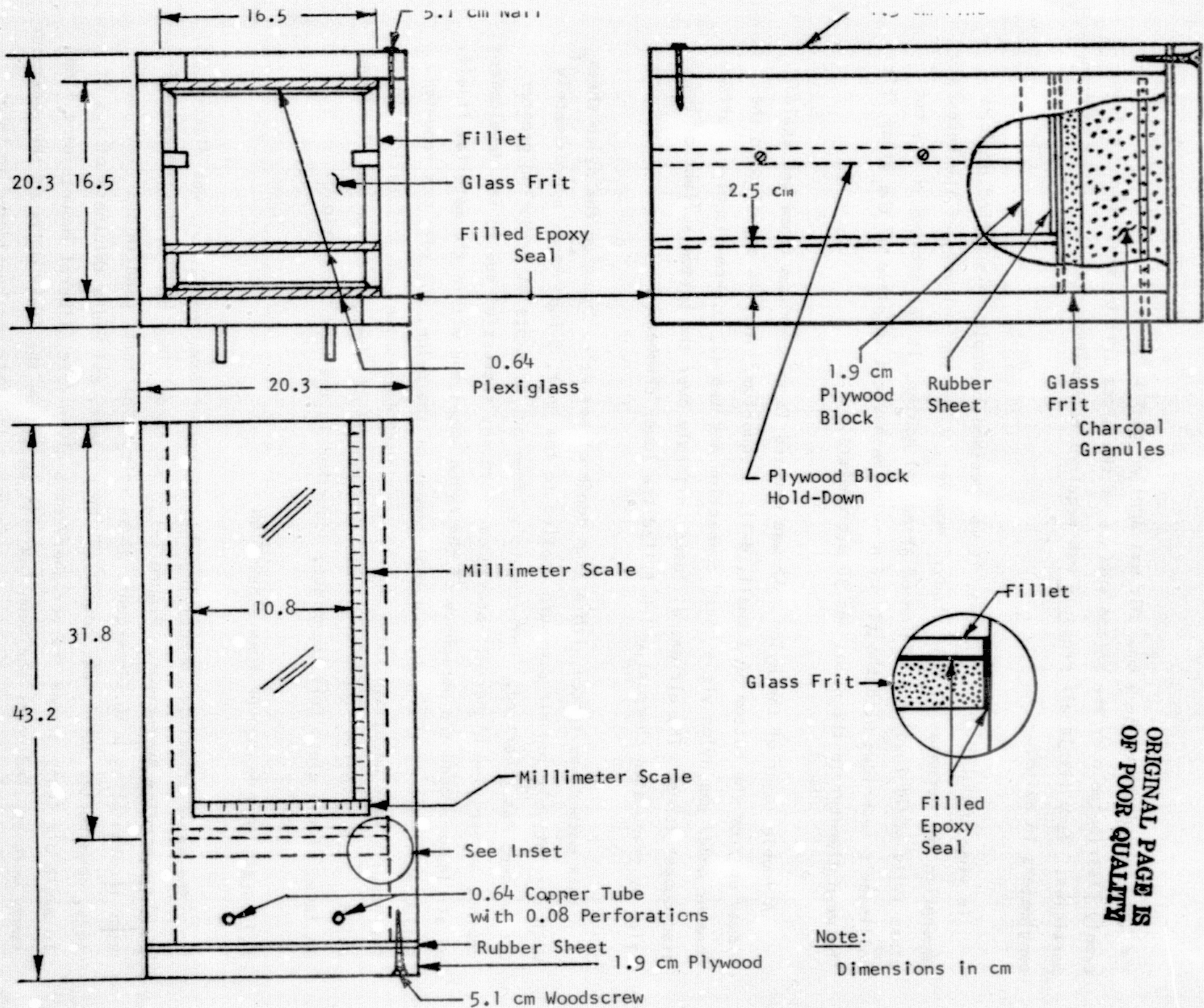
A double layer of the nylon mesh was mounted in an aluminum frame and sealed midway up from the bottom of a small, 8-litre aquarium. Air was supplied to the chamber under the nylon via a "tee" connection and two (2) 0.6-cm-diameter, perforated copper tubes. The air was diffused uniformly over the bottom surface of the nylon by granulated charcoal which filled the lower chamber.

This method was tested with a 3-cm depth of sea water lying on the nylon sheet. With a relatively low air pressure applied to the unit, a foam layer approximately 0.6 cm deep was generated. Unfortunately, however, attempts at producing greater depths, by applying higher air pressures, were not successful due to the development of air leaks around the periphery of the nylon sheet and within the material itself. Following repair of the leaks and replacement of the nylon, the test was repeated. The results were unsatisfactory, due to continued development of perforations in the nylon. As a result of these problems, this method of foam generation was abandoned in favor of the glass frit technique, described in the next Subsection.

## 2.7 GLASS FRIT METHOD OF FOAM GENERATION

The basic principle, underlying this method of foam generation, was discussed in the preceding Subsection. Figure 2-1 shows three views of a typical foam generator incorporating a 16.5-cm-square glass frit. The frits used in the five generators, constructed during the course of the project, all had a thickness of 1.3 cm. To avoid air leaks around the periphery of a given frit, liberal amounts of filled epoxy were applied under the mounting fillets and on the inner walls of the generator housing, as indicated in the inset in Figure 2-1. This was considered to be an

Figure 2-1 - Layout Showing Foam Generator, using Individual Glass Frit



ORIGINAL PAGE IS  
OF POOR QUALITY



important precaution, since air leaks produce foam bubbles that are much larger than those generated by the glass frit. As shown in the Figure, 0.64-cm-thick plexiglass windows were provided on opposite sides of the generator, to permit examination and photography of the foam profile.

The glass frit foam generators, fabricated during the course of the project, are listed in Table 2-1.

Table 2-1

GLASS FRIT FOAM GENERATORS FABRICATED DURING PROJECT

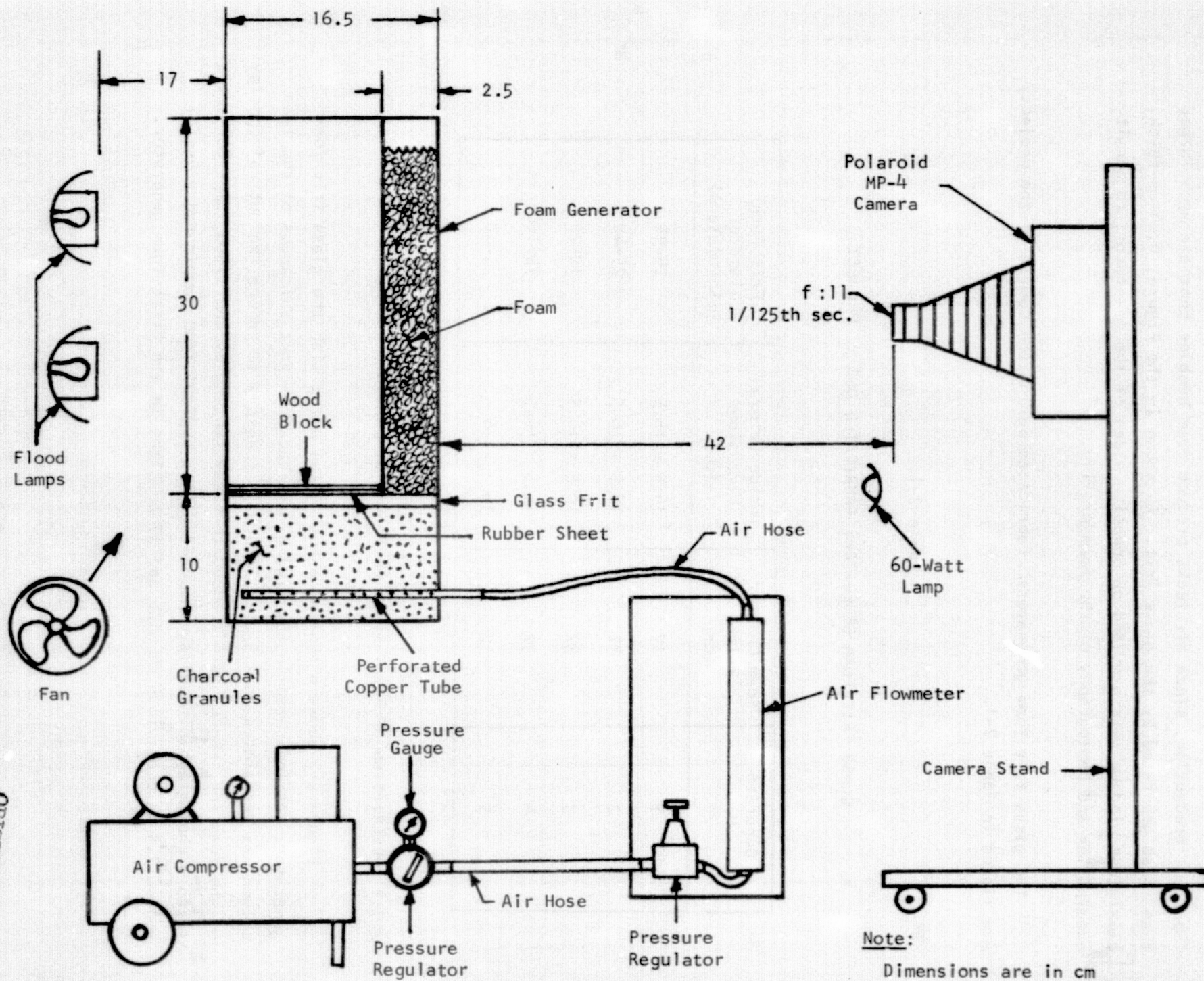
Generator No.	Foam Chamber Height (cm)	Inside Lateral Dimensions (cm)	Frit Pore Diameter (micrometers)
1	17	16.5 x 16.5	25-40
2	32	16.5 x 16.5	25-40
3	32	16.5 x 16.5	10-20
4	32	16.5 x 16.5	70-100
5	32	36 x 36	25-40

2.7.1 DESCRIPTION OF FIRST GLASS FRIT FOAM GENERATOR

Figure 2-2 shows a typical experimental setup with the glass frit foam generator. As indicated in the Figure, the back-to-front thickness of the foam column was restricted to 2.5 cm. This was necessary to reduce the optical opacity of the foam and, hence, permit adequate back-lighting by the flood lamps for satisfactory photographic results. Accordingly, a typical foam sample had a useful volume 2.5 cm deep, 16.5 cm wide and 17 cm high, in the first foam generator.

Figure 2-2 Foam Generator Experimental Setup

2-8



ORIGINAL PAGE IS  
OF POOR QUALITY

During a typical experiment, an initial water depth of 5 cm was used in the generator. The sea water needed for these investigations was obtained 45 minutes before high tide, from the end of a 70-meter pier in the harbor in Swampscott, Massachusetts. The water appeared to be relatively free of foreign matter. It was transported in plastic 19-litre containers and used within 4 to 24 hours. Typical values of salinity, temperature and conductivity, during measurements, were 29 ‰, 21°C and 40,000 micromhos per cm, respectively.

The applied pressure ranged from 0 to 0.8 Kg/cm<sup>2</sup>. Figure 2-3 shows the relationship between applied pressure and foam height in the first foam generator. The plot shows that the maximum foam height "saturates" at approximately 12 cm. This is due to an insufficient volume of water in the generator. It was found, in subsequent experiments, that a higher initial water level results in a higher saturation level.

It should be mentioned that the pressure regulator on the paint sprayer-type compressor could not maintain a sufficiently steady air pressure in the foam generator, for a constant head of foam. Accordingly, a second regulator was added, to stabilize the pressure variations. This unit was a Nullmatic Pressure Regulator, Model 40-200, manufactured by the Moore Products Co. An air flowmeter (Model No. 10K2735C, manufactured by Fischer and Porter Co.) with an air flow capacity of 2.7 litres per second (5.8 ft<sup>3</sup>/min) was placed in series with the regulator. Unfortunately, this device did not register any readings during most of the foam generator experiments. It is likely that, in most cases, the volume of air used was too small to actuate the flowmeter.

#### 2.7.2 PHOTOGRAPHIC METHOD - FIRST FOAM GENERATOR

Initial attempts to photograph the foam bubbles involved experimentation with a variety of different lighting arrangements. The arrangement producing the best uniform illumination of the bubbles is described below.

The first lighting tests had shown that the layer of foam should not be thicker than about 2.5 cm, to allow sufficient light to penetrate the foam from the rear and clearly define the front foam bubbles. As mentioned in Section 2.7.1, the foam

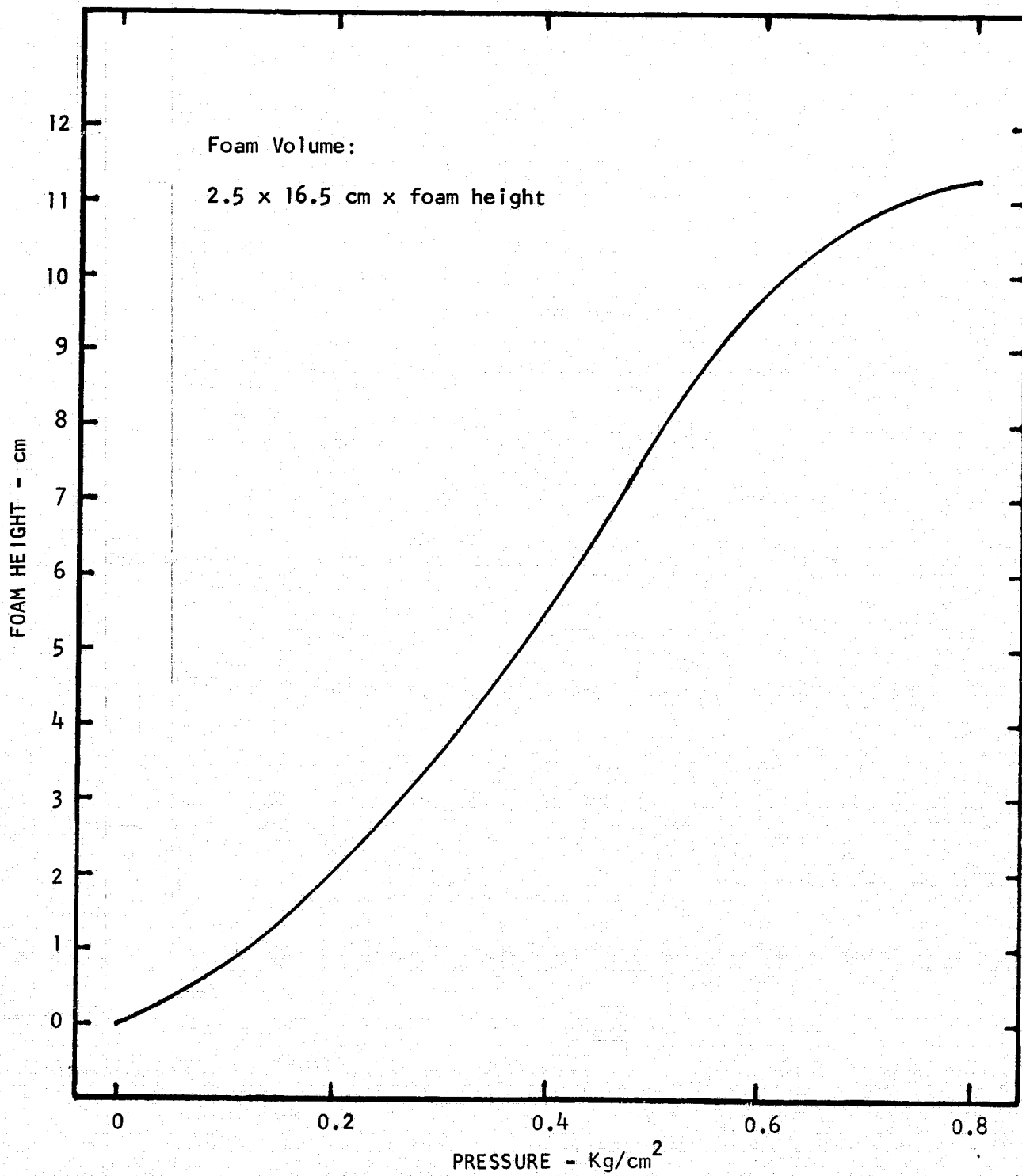


Figure 2-3 Foam Height as a Function of Applied Air Pressure (First Foam Generator)

generator was modified to produce a narrow, rectangular volume of foam 2.5 cm deep x 16.5 cm wide, and up to 17 cm high, depending on the applied air pressure.

A Polaroid Model MP-4 camera, using Polaroid Type 105 positive/negative film, was positioned so that its lens was 23 cm from the front plexiglass window. A millimeter scale was placed along the lower and right-hand edges of the window, to allow accurate determination of foam bubble diameters in the enlarged photographs. In addition to the rear flood lamp, an identical lamp was mounted above the foam surface and a small incandescent lamp was positioned between the camera and the front of the box to illuminate the scale and the front surface of the foam. To reduce the depth of field, the largest lens aperture available (f:4.5) was used; the fastest shutter speed available (1/125 second) was found to be satisfactory in stopping bubble motion. Though the initial lighting experiments involved trying several gelatin filters singly or in combination, including red and polarizing filters, in front of the lens, no filters were used in connection with any of the subsequent experiments. Cardboard shields were placed across the front plexiglass window just above the top of the foam layer being photographed; when the foam layer was relatively low, the shields prevented light from the rear flood lamp from shining over the top of the foam and directly into the camera lens.

### 2.7.3 DESCRIPTION OF LARGER FOAM GENERATORS

The larger glass frit foam generators are designated as Nos. 2, 3 and 4 in Table 2-1. They were identical to the first generator, except that the height of the foam chamber was 32 cm instead of 17 cm.

Thirty-eight litres of sea water were taken in late December 1974 from the end of Swampscott Pier. As mentioned in Section 2.7.1, the water was taken during the 45 minutes immediately preceding high tide, and appeared to be fairly clean. At the time the samples were taken, the temperature of the water was 3.8°C, its salinity was 30.6 ‰, and its conductivity was about 28,550 micromhos per centimeter.

In each of the taller foam generators, the initial water level was 7 cm. As was expected, the level of foam achieved with a given air pressure was strongly dependent on the porosity of the frit used. No saturation effect was noted — all

three of the foam generators could generate foam heights exceeding the height of the generator, without using air pressures exceeding  $0.63 \text{ Kg/cm}^2$ . As an indication of the foaming ability of each frit, the following air pressures were required to generate 30 cm of foam:

10-20 micrometer frit:  $0.63 \text{ Kg/cm}^2$

25-40 micrometer frit:  $0.42 \text{ Kg/cm}^2$

70-100 micrometer frit:  $0.07 \text{ Kg/cm}^2$

It should be noted that the foam volumes generated in each case were 2.5 cm deep x 16.5 cm wide x 30 cm high and did not fill the entire foam chamber.

#### 2.7.4 PHOTOGRAPHIC METHOD - LARGER FOAM GENERATORS

Because these three foam generators were much taller than the first foam generator, a new camera position, with lens settings and lighting arrangements different from those described in Section 2.7.2, had to be found which would allow the increased foam height to be included in the photograph. Following some experimentation, the camera was positioned so that its lens was 42 cm from the front plexiglass window, as shown in Figure 2-2. To illuminate uniformly the higher foam levels, two white flood lamps were mounted vertically, about 17 cm behind the rear plexiglass window. To keep the rear plexiglass window from being overheated by the hot flood lamps, an electric fan was placed close by to cool the rear of the generator. There was no overhead flood lamp, as was used with the first foam generator. However, a small incandescent lamp was used to illuminate the front surface of the foam bubbles, and the new millimeter scales. These had 0.5 mm graduations and were placed along the bottom and left side of the front plexiglass window. A scale with 1 mm graduations was placed adjacent to the right edge of the front plexiglass window. Also, cardboard shields were again placed across the front plexiglass window, just above the top of the foam layer being photographed; when the foam layer was relatively low, the shields prevented light from the rear flood lamps from shining directly into the camera lens. Photographs were again taken with the Polaroid MP-4 camera, without filters, with a shutter speed of  $1/125$ th sec. The higher light levels, however, necessitated using a lens aperture of f:11.

## 2.7.5 DESCRIPTION OF MULTIPLE-FRIT FOAM GENERATOR

This foam generator is designated as No. 5 in Table 2-1. The purpose of this unit was to determine the volume of foam that could be generated by a multi-frit array, bearing in mind the full-scale 1.2 x 1.2 meter foam generator that would be, eventually, fabricated for use in the NASA Langley Research Center roof-top wave tank. Provision was made for the use of four (4) 16.5 x 16.5 cm glass frits in this unit. Unfortunately, only three were available at the time of completion of the generator; accordingly, one of the positions was blanked off with a sheet of plexiglass. One of the frits was defective and passed only a small amount of air, under maximum applied pressure. Thus, the 36 x 36 cm working area, in this generator, was fed by air from only two frits. As indicated in Table 2-1, the pore diameters in these frits were in the range 25-40 micrometers.

It should be mentioned that, unlike the first four glass frit foam generators, this generator was fabricated entirely from 0.64-cm plexiglass. The frits, themselves, were sealed with filled epoxy in a square, U-channel aluminum frame. Air leakage, through the joints between the frits, was prevented by cementing 1.9-cm-wide aluminum strips along the joints, on both sides of the assembly. Filled epoxy was also used in these seals.

Thirty-eight litres of clean sea water were taken, in early February 1975, from the end of Swampscott Pier, 45 minutes prior to high tide. At the time of sampling, the water temperature was 1.5°C, the salinity was 32.5 ‰, and the conductivity was about 28,500 micromhos per centimeter.

Since the objective, with this generator, was to determine the abundance of foam with a multi-frit unit, no photographs were taken of the foam. The results obtained with this generator are discussed in Section 3.

## Section 3

### PHYSICAL AND MICROWAVE CHARACTERISTICS OF OCEAN FOAM

#### 3.1 RESULTS WITH FIRST FOAM GENERATOR

##### 3.1.1 PREPARATION OF PHOTOGRAPHS

The negatives of those foam photographs chosen for further study were enlarged by Mr. Don Harper, a professional photographer with Environmental Research and Technology, Inc. Lexington, Massachusetts. Large 20 x 25 cm positive prints were produced to facilitate the study of bubble size and distribution. A standard enlarger was used, together with Kodak Kind 2200 printing paper, an experimental product that produces a non-glossy print and which readily accepts pencil or pen marks. Considerable care was necessary during the printing process, due to the presence of non-uniform brightness in the negative.

##### 3.1.2 ANALYSIS OF PHOTOS FOR BUBBLE SIZE DISTRIBUTION

Initial examination of the foam photographs revealed that bubble size and distribution were, principally, a function of vertical position in the foam layer and independent of horizontal position in the foam area. Consequently, it was decided to measure and count bubbles in an arbitrarily located 2.5-cm-wide vertical column, in the scale of the photograph. The column was clearly marked on the photograph with a sharp black pen. The column was divided into rectangular blocks each 1 cm high, also in the scale of the photograph, beginning at the foam-water interface, if visible, or at the top edge of the scale, located across the bottom of the plexiglass window, if the interface was not visible. It was noted that the foam-water interface, where visible, was quite distinct; below it was free standing water, and above it was the slightly darker, foam layer comprised of bubbles  $\leq 0.5$  mm in diameter. There appeared to be no gradual merging of water into foam but a relatively sharp discontinuity, no more than 1 to 2 mm, in width, where the water suddenly became foam.



A sample photograph, showing foam produced by the first generator, is reproduced in Figure 3-1. The bubbles, appearing in the marked off column, were measured and classified in terms of diameter with the aid of a lighted magnifying glass. After being measured, a given foam bubble was marked with a pencil to avoid counting it again. The record sheet used in recording the number of foam bubbles, of given diameter, in each "box" of the photograph, is shown reproduced in Figure 3-2.

### 3.1.3 BUBBLE SIZE DISTRIBUTIONS

The number of bubbles in a predetermined diameter range, in each rectangular area, in the vertical column drawn on the photograph, was tabulated and plotted as a function of the depth below the foam-air interface. Thus, the count consisted of the number of bubbles within the top 1 cm, the number between the 1 to 2 cm depths, the number between the 2 to 3 cm depths, etc. The total number of bubbles in each size range, in the entire vertical column, was also tabulated and presented in the upper portion of each plot. Though this number varied with different heights of foam, it was needed to permit calculation of the percentage that each bubble size comprised of the total number of foam bubbles. Figures 3-3, 3-4 and 3-5 show plots of foam bubble counts as a function of bubble diameter and depth below the surface, for different applied air pressures. The mean bubble diameters, for various depths, are also shown in the plots. These were calculated by the following formula, given in Miyake and Abe<sup>2</sup>:

$$\bar{d} = \sqrt[3]{\frac{\sum d^3}{\sum n}}$$

where,

d is the diameter of each bubble,

and n the number of bubbles of that diameter.

During the course of tabulation, bubble diameters were placed in quantized ranges and not counted individually by exact size; the upper diameter in each range was arbitrarily selected as 'd' for the above equation. The number of bubbles for that diameter range was 'n'. In the computations,  $d^3$  was calculated for each diameter range and then multiplied by the number of bubbles counted in that range.

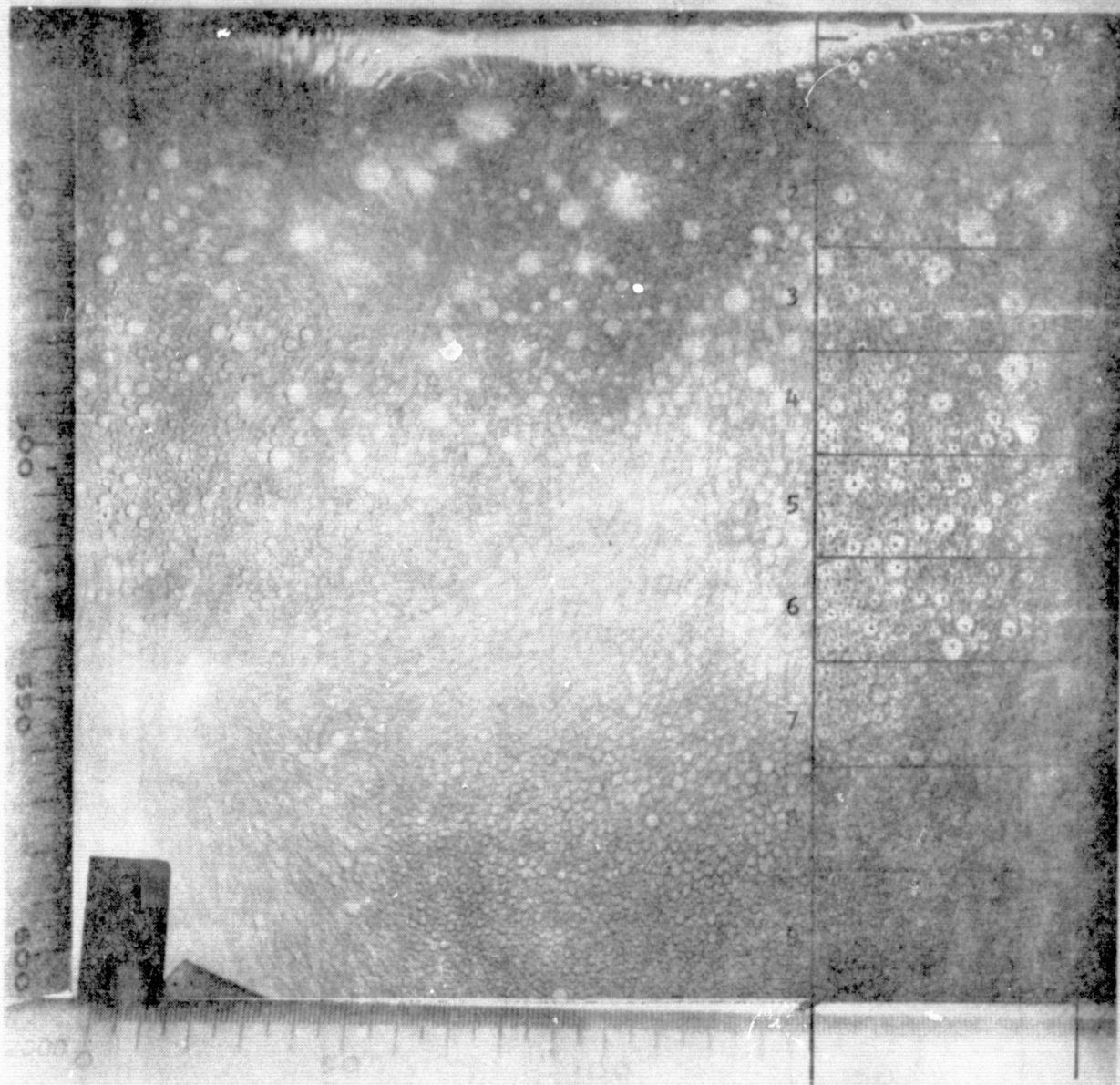


Figure 3-1 Enlarged Photo of Sea Water Foam, 25-40 Micrometer Glass Frit

**ORIGINAL PAGE IS  
OF POOR QUALITY**

OCEAN FOAM BUBBLE DIAMETERS

Expt. No. _____ Date: _____ Photo No. _____ Box No. on Photo _____	$\leq 0.5$ mm	0.6 - 1.0 mm	1.1 - 1.5 mm	1.6 - 2.0 mm
2.1 - 2.5 mm	2.6 - 3.0 mm	3.1 - 3.5 mm	3.6 - 4.0 mm	4.1 - 4.5 mm
4.6 - 5.0 mm	5.1 - 5.5 mm	5.6 - 6.0 mm	6.1 - 6.5 mm	6.6 - 7.0 mm
7.1 - 7.5 mm	7.6 - 8.0 mm	8.1 - 8.5 mm	8.6 - 9.0 mm	9.1 - 9.5 mm

Figure 3-2 Sheet for Recording Foam Bubble Diameters, Counted in Selected Area on Enlarged Photo

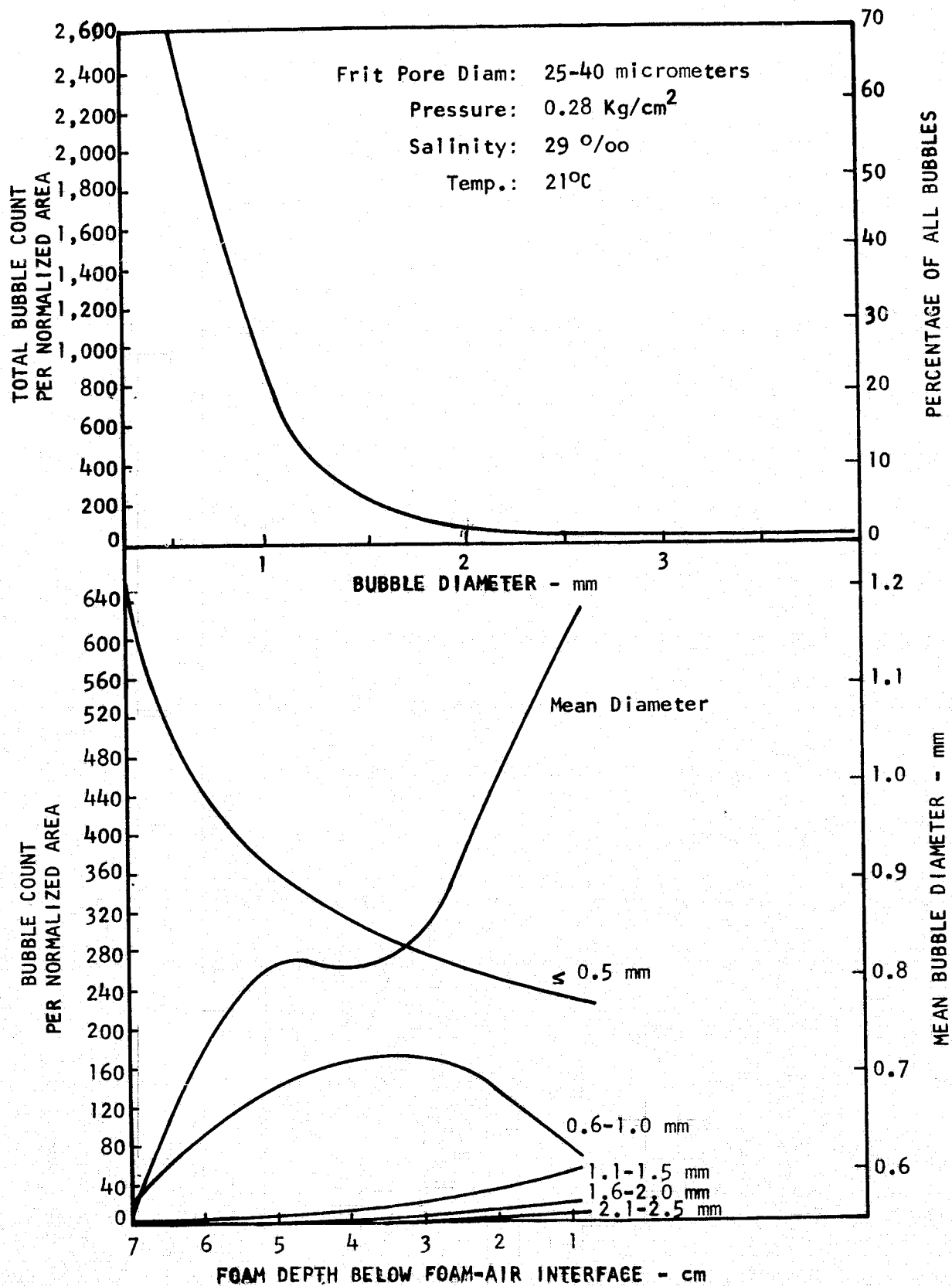


Figure 3-3 Foam Bubble Count as a Function of Bubble Diameter and Depth Below Surface

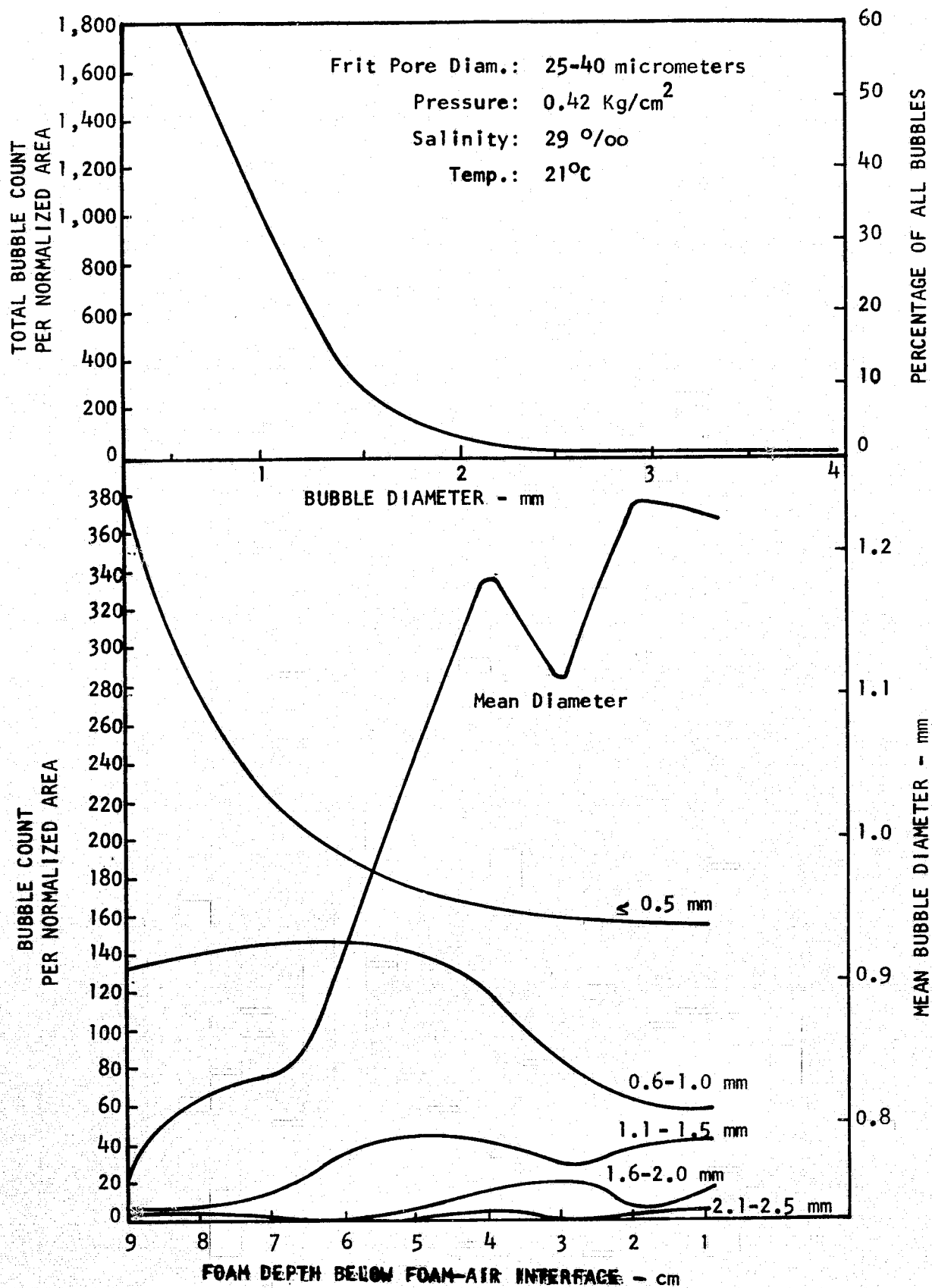


Figure 3-4 Foam Bubble Count as a Function of Bubble Diameter and Depth Below Surface

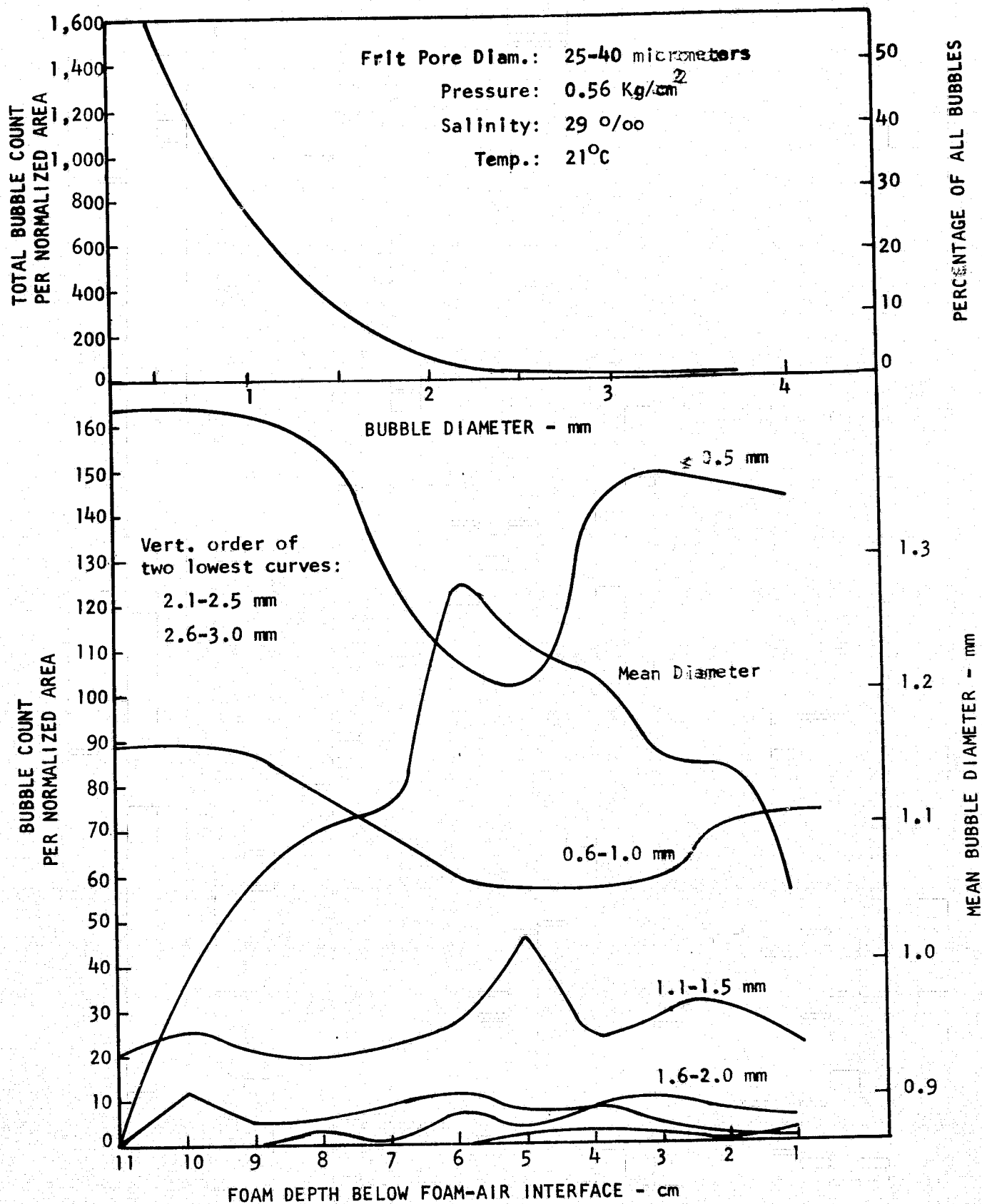


Figure 3-5 Foam Bubble Count as a Function of Bubble Diameter and Depth Below Surface

This procedure was applied to the other diameter ranges, and the sum of the results from all these ranges is the  $\sum d^3$  in the above equation.  $\sum n$  is the total number of bubbles, of all sizes, counted in all the diameter ranges previously considered. The values, thus obtained for  $\bar{d}$ , are shown in the above Figures. The remaining plots, produced from data obtained with the first foam generator, are presented in Appendix A.

When greater depths of foam were to be photographed, higher applied air pressures were required. However, increasing the air flow and pressure tended to exaggerate the existing sporadic air pressure variations. These, in turn, tended to affect the observed bubble distribution as a function of depth in the foam layer, causing the 'noisy' plots of the mean and individual bubble diameters for greater foam depths; however, the number of photographs studied was sufficiently large, statistically, to smooth the data distribution.

The plots give self-consistent results when compared with ocean foam data obtained by Miyake and Abe<sup>2</sup>. The average mean bubble diameter was about 0.88 mm, corresponding to a chlorinity of approximately 18 ‰, as determined from op. cit. This chlorinity value, is consistent with the lower salinity of 29 ‰, exhibited by the Swampscott ocean water used in this study, as determined with a salinometer at the ocean. The open ocean has a salinity of approximately 35 ‰ and, since the sample of ocean water used in the present experiment was taken within 70 meters off shore, the fact that it was slightly less saline is not unexpected, particularly since the Saugus and Pines River estuaries are located only 3 to 4 miles away from the Swampscott pier.

The appearance of the bubble count vs. bubble diameter plots are very similar for each photograph and compare closely with Figure 4, op. cit., for an interpolated chlorinity of 18 ‰. Hence, the bubble analysis method is evidently suitable and credible, since it duplicates results obtained by other researchers, using different methods and equipment.

In all photographs, the major components of the foam were bubbles  $\leq 0.5$  mm in diameter, comprising 56 - 75% of all bubbles counted. Bubbles 0.6 - 1.0 mm in diameter comprised 20 - 34% of all bubbles counted, and bubbles 1.1 - 1.5 mm in diameter constituted from 3 to 10% of the total sample. The relative proportions were found to be a function of pressure and, therefore, of foam height, with the lower pressures

producing a higher percentage of the smallest bubbles. This was expected, since the greater foam heights were observed to have a larger number of relatively large bubbles - > 1.5 mm in diameter.

The distribution of the smallest bubbles ( $\leq 0.5$  mm) with foam depth, roughly follows a decaying exponential relationship, dropping from a high count, in the lowest centimeter thickness of foam, just above the foam-water interface, to roughly 40% of this value through the uppermost 2-3 cm of foam. For foam depths greater than about 7 cm, the number of bubbles 0.6-1.0 mm in diameter peaks from 3-6 cm below the top of the foam layer and then decreases by roughly 50% in the top 1 cm of foam. For foam depths less than about 6 cm, the 0.6-1.0-mm bubbles slowly increase in number from the bottom of the foam layer to the top, asymptotically approaching a constant value in the upper 2-3 cm of foam. The 1.1-1.5 mm-diameter bubbles seem to follow the same distribution pattern as the 0.6-1.0-mm bubbles, even though their total number is about 22% of the total number of 0.6-1.0-mm bubbles. Larger bubbles will occur only with foam depths greater than approximately 5 cm; the number of these larger bubbles appears to increase asymptotically, approaching a constant value toward the foam-air interface.

A conclusion that may be drawn from this data is that the number of bubbles of a given size, at a given depth in the foam, is a function of the foam height. For example, for small foam heights, about 90% of the bubbles in the bottom centimeter of foam were  $\leq 0.5$  mm in diameter. For greater heights, these bubbles comprised only about 50% of the total number, with a higher proportion of larger bubbles making up the difference. Similarly, other distributions of bubble size with depth, as a function of total foam height, were noted.

Figure 3-6 shows the distribution of bubble diameters in foam of differing depths. This plot combines data from twelve photographs, taken of foam ranging in depth from 3 cm to over 10 cm. It is clear that for greater foam heights (> 7 cm), there is a larger relative percentage of larger bubbles. This fact has important implications in the determination of the particular artificially-generated foam layer most similar to natural ocean foam.



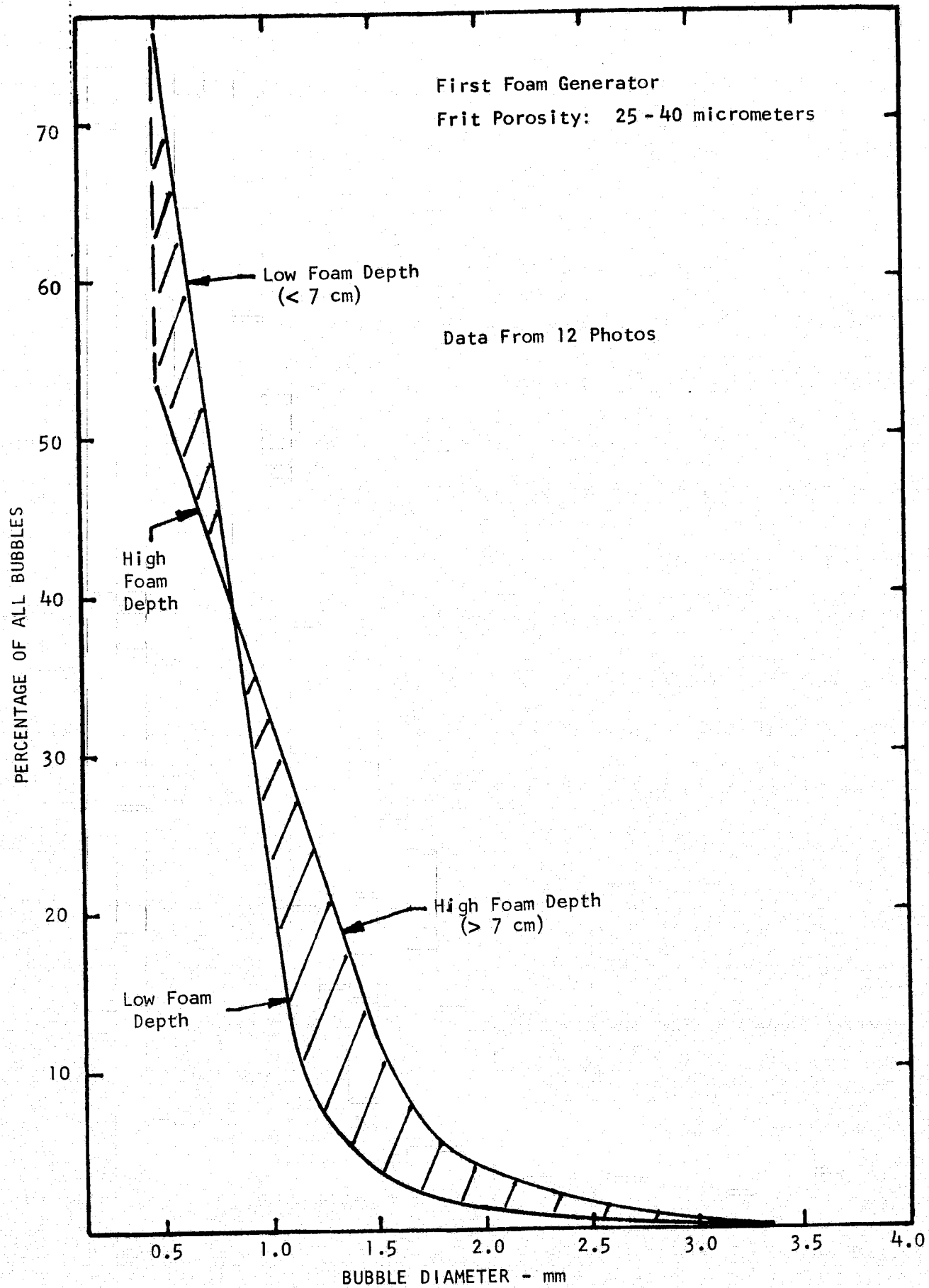


Figure 3-6 Percentage of All Bubbles versus Bubble Diameter, for 25-40 Micrometer Frit

Figures 3-7 through 3-9 show the combined data of twelve (12) photographs of foam of varying heights. Figure 3-7 shows that the relative number of very small bubbles ( $\leq 0.5$  mm in diameter) at various depths in the foam is greatest for low foam heights and lowest for high foam heights. Figure 3-8 shows that the relative number of slightly larger size bubbles ( $0.6-1.0$  mm in diameter) drops off sharply at increasing foam depths for low foam heights and that it remains fairly constant at a higher range of values for initially greater foam heights. Figure 3-9 shows that the relative number of intermediate to larger size bubbles ( $1.0-1.5$  mm in diameter) is greatest for the upper 7-8 cm of high foam samples and decreases at greater depths for lower initial foam heights. A similar pattern is observed for even larger diameter bubbles.

#### 3.1.4.4 AIR AND WATER CONTENT OF OCEAN FOAM

In order to determine the dielectric properties of ocean foam, its air and water content have first to be measured. Accordingly, a graduated 50 ml beaker, was used to take samples of foam from various depths in the foam layer produced by the first foam generator. The beaker was then used to measure the volume of water remaining after dissipation of the foam. The glass frit in this generator had a pore diameter in the range 25-40 micrometers. The full  $16.5 \times 16.5$  cm area of the frit was used with applied air pressures of up to  $0.050 \text{ kg/cm}^2$  to generate foam ranging up to 51 cm in height.

Sea water samples were obtained approximately one-half hour before high tide from the Swampscott pier. The water samples appeared clear and quite free of suspended particles and other visible substances. At the time the samples were taken the water temperature was  $9.0^\circ\text{C}$ , its salinity was  $29.2$  ‰, and its conductivity was about  $813,600 \text{ micromhos/cm}$ .

The laboratory investigation of the water and air content of foam was performed within three (3) hours of the time the water samples were taken. At the time of the foam generation and sampling, the water temperature was  $13.0^\circ\text{C}$ . When the generated foam height was greater than 77 cm, it was possible to obtain foam samples at varying depths, referred to as "Top", "Middle", and "Bottom". The Top sample was taken from the upper 4 cm of foam, the Middle from the middle 4 cm of foam and

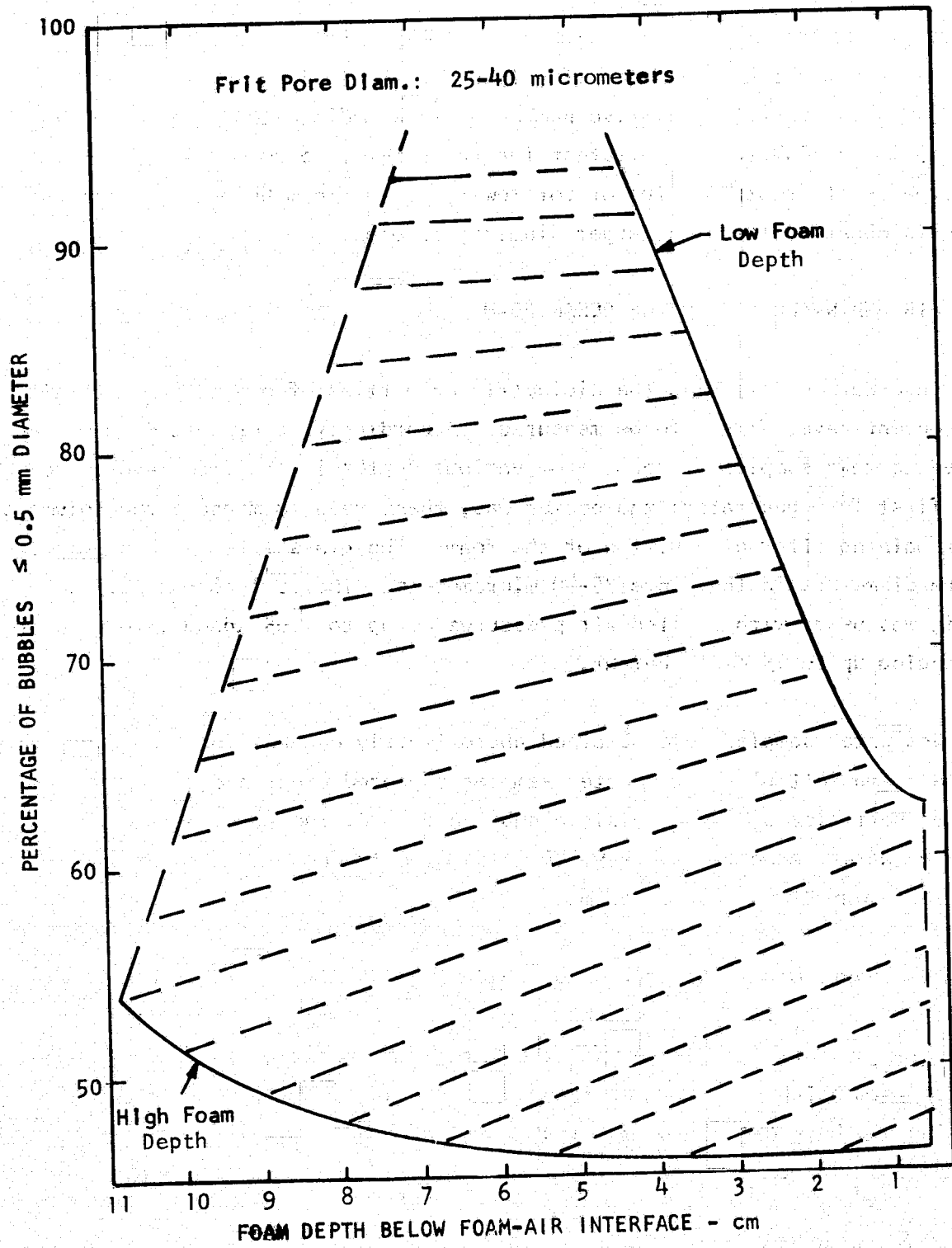


Figure 3-7 Percentage of Foam Bubbles with Diameters  $\leq 0.5$  mm (First Foam Generator)

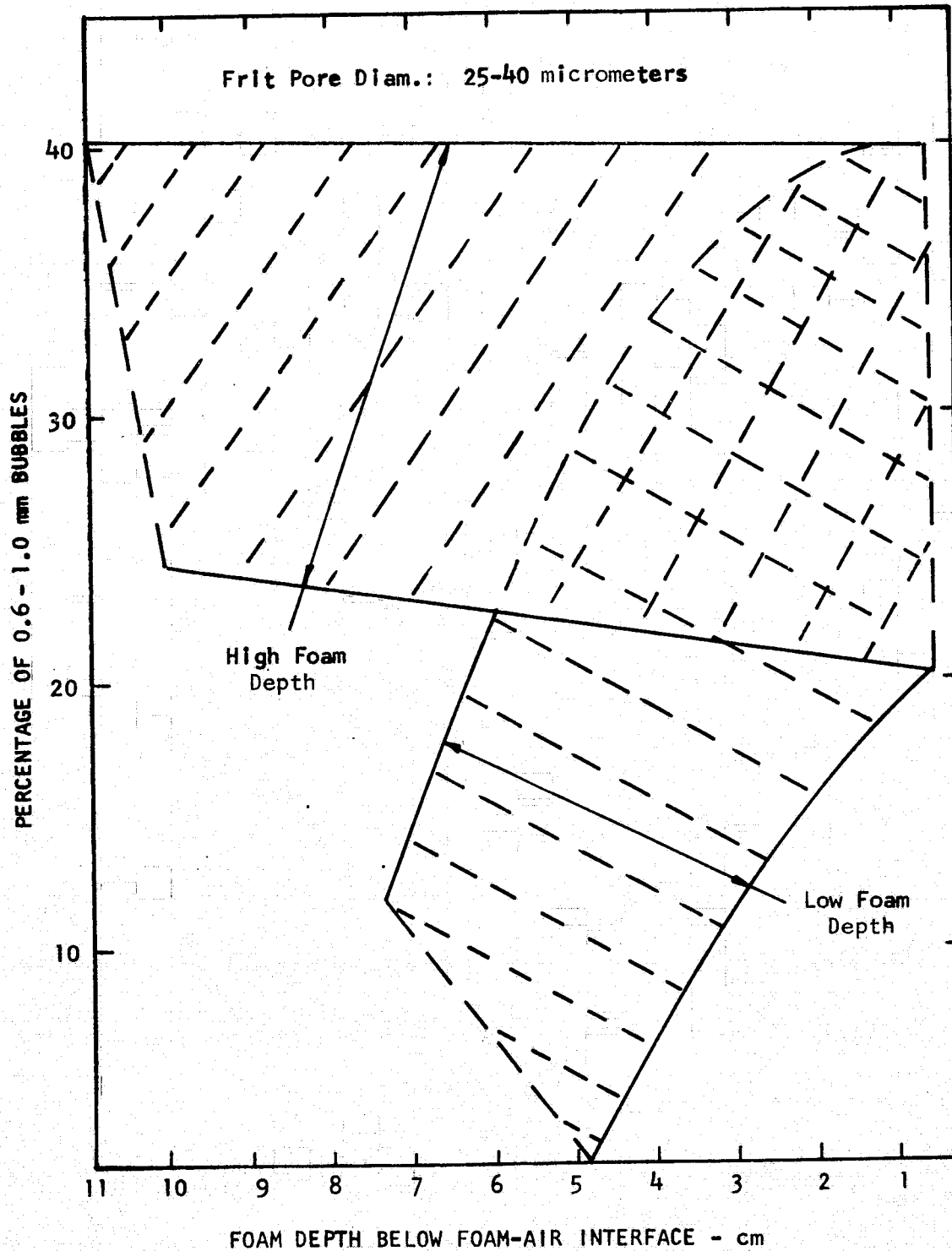


Figure 3-8 Percentage of 0.6 - 1.0 mm Diameter Foam Bubbles (First Foam Generator)

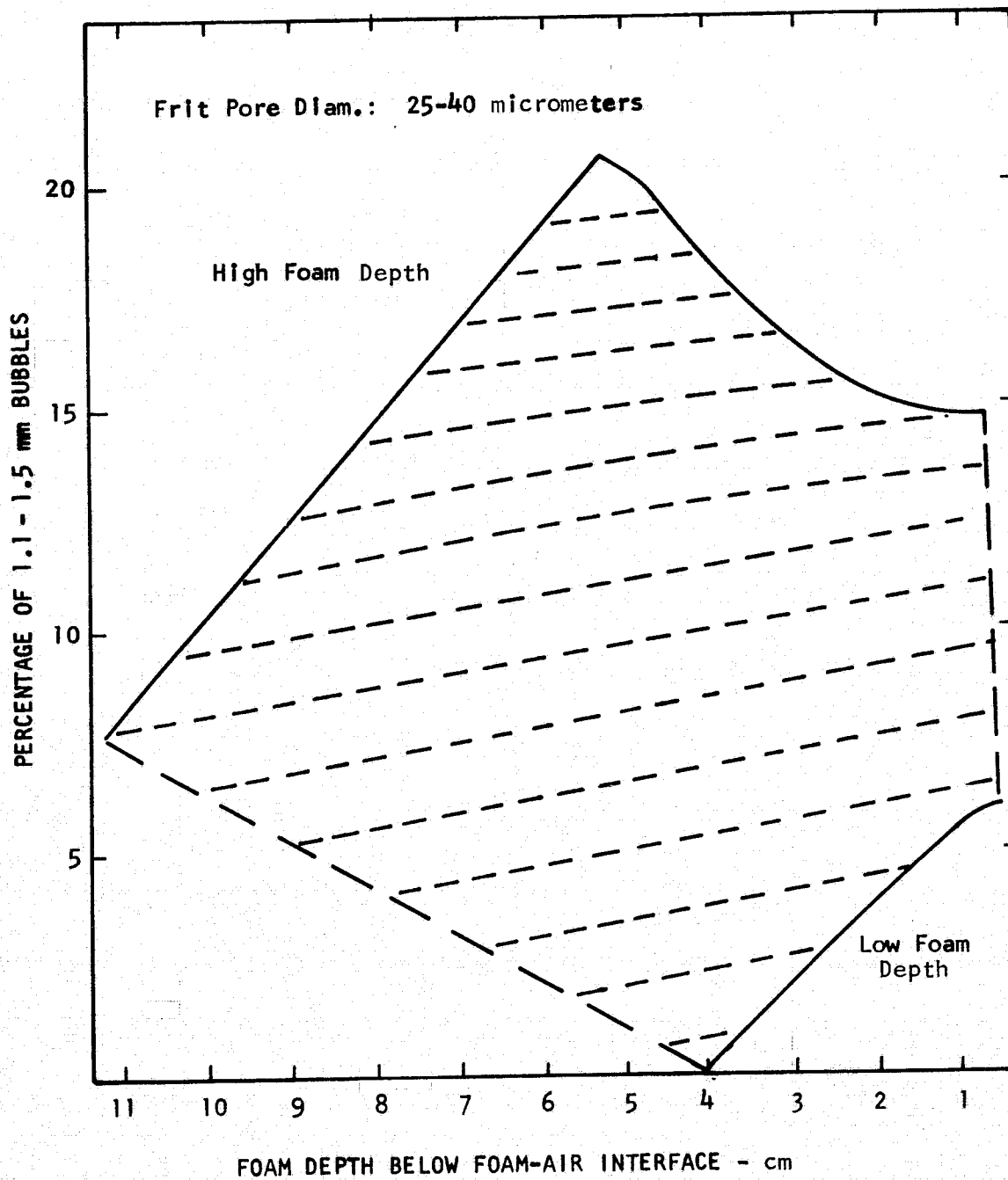


Figure 3-9 Percentage of 1.1 - 1.5 mm Diameter Foam Bubbles (First Foam Generator)

the Bottom sample from the bottom 4 cm of foam, just above the foam-water interface. The beaker was positioned horizontally at the proper depth in the foam and, immediately thereafter, moved toward the tank window. It was held against the window as it was moved up, out of the foam, and was not turned upright until it emerged from the foam. If the beaker were not filled to the top with foam, the sampling was repeated. The foam in the beaker dissipated within a few seconds after the sample was taken.

The results, presented in Figure 3-10, show that the average water content is relatively constant at 35% by volume, for a total foam height greater than 6.5 cm and is a linear function of total foam height for heights less than 6.5 cm.

It is interesting to note that the water content in the Top layer is approximately 28%; in the Middle layer it is approximately 36% and in the Bottom layer it ranges between 39 and 42%.

A second set of foam samples were taken at a temperature of 18.4°C, to determine the effect of temperature on the amount of foam generated. It was noted that, over this 5.4°C temperature interval, the foam height was essentially temperature independent. This is consistent with results obtained by Miyake and Abe<sup>2</sup>.

### 3.1.5 DIELECTRIC PERMITTIVITIES AND ELECTRICAL SKIN DEPTHS OF OCEAN FOAM

The relative dielectric permittivities of foam can be determined by considering it to be a porous medium, as discussed in Porter and Wentz<sup>3</sup>. The dielectric permittivity,  $\epsilon$ , of a material is defined by the complex relation,  $\epsilon = \epsilon' - j\epsilon''$  in which  $\epsilon'$  and  $\epsilon''$  are the real and imaginary parts of the permittivity, respectively. Using data from that report, the following relative dielectric permittivities are obtained for sea water at a frequency of 1.4 GHz, for a salinity of 29 ‰ and temperature of 286°K:  $\epsilon' = 74.5$  and  $\epsilon'' = 56.4$ .

In the porous medium model,

$$\epsilon'_{\text{foam}} = V_a \epsilon'_a + V_w \epsilon'_w \quad (3-1)$$

and,

$$\epsilon''_{\text{foam}} = V_a \epsilon''_a + V_w \epsilon''_w \quad (3-2)$$

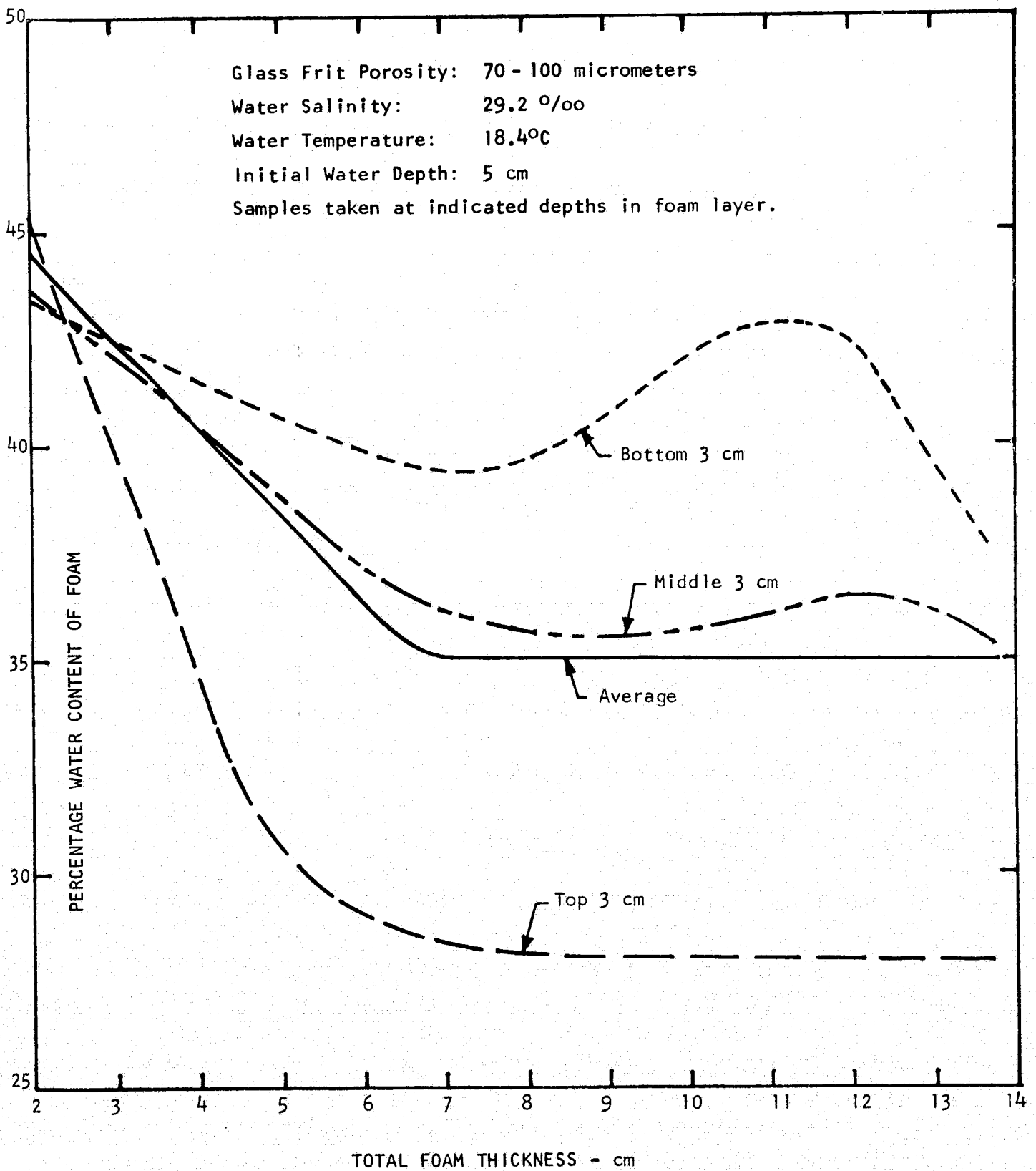


Figure 3-10 - Percentage Water Content of Ocean Foam as a Function of Total Foam Thickness

Since  $e_a' = 1$ , and  $e_a'' = 0$ , we have for foam,

$$e_f' = V_a + V_w e_w' \quad (3-3)$$

and,

$$e_f'' = V_w e_w'' \quad (3-4)$$

$V_a$  and  $V_w$  are the average relative volumes, respectively, of air and water to the total foam volume.

As given by von Hippel<sup>4</sup>, the attenuation factor is,

$$\alpha = \frac{2\pi}{\lambda_0} \left[ \frac{1}{2} e' \left\{ \sqrt{1 + \tan^2 \delta} - 1 \right\} \right]^{\frac{1}{2}} \quad (3-5)$$

where;  $\lambda_0$  is the wavelength of the radiation in free space  
and  $\tan \delta$  is the loss tangent.

The attenuation distance  $1/\alpha$ , or skin depth, is the distance through the dielectric over which the field strength of the radiation decays to  $1/e$ , or 0.368 of its original value.

Table 3-1 shows the results of calculations of the above parameters for three (3) depths of foam, at a frequency of 1.4 GHz.

It will be noted that  $e_f'$  ranges from 33.6 to 26.7, over the foam depth range of 1.5 to greater than 7 cm. The imaginary part,  $e_f''$ , ranges from 25.0 to 19.7 over the same foam depth. Also, the inverse of the attenuation factor ranges from 1.67 to 1.89 cm over this range of foam depth. From these results, it appears that, for any layer of foam at this temperature and salinity, with a depth greater than about 1.68 cm, the field strength of radiation propagating through it would decay to more than  $1/e$  of its original value. Under these conditions, the foam layer could be considered as a semi-infinite medium at 1.4 GHz. At higher frequencies, this critical depth would decrease.

It should be noted that the results, presented in Table 3-1 are supplemented by more definitive findings presented in Table 3-2, in Section 3.2.5.



Table 3-1

ELECTRICAL CHARACTERISTICS OF OCEAN FOAM AT 1.4 GHz  
(Data from First Foam Generator)

Foam Thickness (cm) →	1.5	2	≥ 7
$V_w$ (%)	44.4	43.5	35.0
$e_f'$	33.63	32.97	26.73
$e_f''$	25.04	24.53	19.74
$\tan \delta$	0.746	0.744	0.739
$\alpha \left( \frac{1}{\text{cm}} \right)$	0.598	0.592	0.530
$\frac{1}{\alpha}$ (cm)	1.67	1.69	1.89
DB loss/cm	5.19	5.14	4.60

## Nomenclature:

- $V_w$  (%) - average percentage volume of water in the entire foam layer
- $e_f'$  - real part of the relative dielectric permittivity of foam
- $e_f''$  - imaginary part of the relative dielectric permittivity of foam
- $\tan \delta$  - loss tangent of the foam ( $e_f''/e_f'$ )
- $\alpha$  - attenuation factor, per cm
- $1/\alpha$  - attenuation distance, or skin depth, cm

## 3.2 RESULTS WITH SECOND FOAM GENERATOR

### 3.2.1 PREPARATION OF PHOTOGRAPHS

A series of photographs were taken of different heights of foam, produced by each of the three (3) different pore-size glass frits, mounted in separate foam generators. These generators are designated by Nos. 2, 3 and 4 in Table 2-1. Two photographs, one of a high level and one of a low level of foam, were then selected as representative of the foam produced by a given glass frit, producing a total of six (6) photographs to be analyzed, two (2) for each of the frits.

The negatives of these foam photographs were again used to make 20 x 25 cm positive prints. Because of supply problems, the photographer was unable to use the highly satisfactory Kodak Kind 2200 printing paper, and was obliged to use Agfa Brovira No. 6, instead, which provided a somewhat glossy surface, and was difficult to write upon with a pen, and impossible to write upon with a pencil.

### 3.2.2 ANALYSIS OF PHOTOS FOR BUBBLE SIZE DISTRIBUTION

Initial examination of these foam photographs revealed that, as in the photographs taken with the first foam generator, the bubble size and distribution were principally functions of vertical position in the foam layer and independent of horizontal position across the face of the foam. In order to photograph the increased height of foam which these new foam generators could produce, the camera was moved farther away from the foam generator. This not only produced a wider field of view in the photographs, but also caused the foam area and the bubbles to appear smaller on the resultant photographs than on those taken with the first foam generator. The smallest bubbles were, therefore, quite difficult to measure and count on the series of photographs taken with the second foam generators.

Because of the smaller plate scale in this series of photographs, it was decided to measure and count bubbles in an arbitrarily-located 2-cm-wide (in the scale of the photograph) vertical column, drawn on the photograph. This column was divided into square boxes, each 2 cm high, also in the scale of the photograph, beginning at the foam-air interface and continuing down to the lowest level of foam clearly depicted in the photograph.

Figure 3-11 shows a photograph of foam generated with the 10-20 micrometer glass frit, which was analyzed following the above-described procedure. Figure 3-12 shows a photograph of foam generated with the 70-100 micrometer frit. The narrow strip of bubbles at the surface was analyzed in an inconclusive attempt to determine surface bubble distribution.

### 3.2.3 BUBBLE SIZE DISTRIBUTIONS

The analysis of the bubble counts, taken with the second series of foam generators, followed the procedure used, with the first foam generator, as described in Section 3.1.3. The resulting plots, shown in Figures 3-13, 3-14 and 3-15, obtained with each porosity frit, particularly in the case of the 25-40 micrometer frit, were comparable in appearance to those obtained earlier with the 25-40 micrometer frit, in the first foam generator. The remaining data, obtained with the second foam generator, are presented in Appendix B. The average mean bubble diameters for each of the three different frits are as follows: 0.88 mm for the 10-20 micrometer frit; 1.28 mm for the 25-40 micrometer frit; and 1.43 mm for the 70-100 micrometer frit.

From an examination of the plotted data, it is evident that the mean bubble diameters are more a function of the porosity of the frit used in a given foam generator than of the chlorinity of the water sample, the data of Miyake and Abe<sup>2</sup>, as referenced in Section 3.1.3, notwithstanding. It should be noted that the larger the pores in the frit, the greater is the air flow into the water. It is clear, though, that for a given initial water level, the 70-100 micrometer frit produced the largest relative number of bubbles with diameters greater than 1 mm. Similarly, for a given initial water level, the 10-20 micrometer frit produced the largest relative number of small bubbles, and the smallest relative number of large foam bubbles. In the presentation of total bubble count versus bubble diameter (the upper plot in the bubble distribution plots), this fact is seen quite clearly. Also of interest, in Figure 3-15, is the shoulder, at a bubble diameter of about 2 mm, for the 70-100 micrometer frit. The exact cause of this higher bubble count, for bubbles between 1.5 and 2.5 mm diameter, is unknown, but it provides a clear indication of the higher percentage of large bubbles produced by the 70-100 micrometer frit.

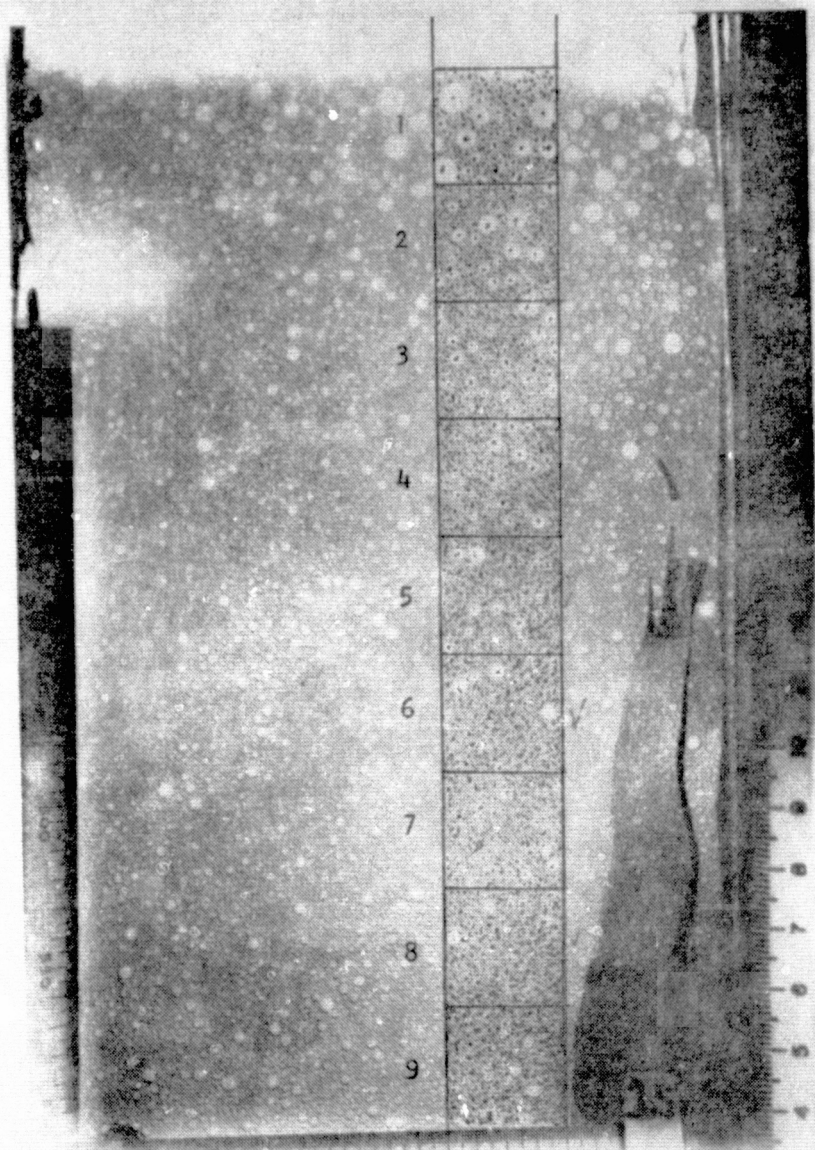


Figure 3-11 Enlarged Photo of Sea Water Foam, 10-20 Micrometer Glass Frit

**ORIGINAL PAGE IS  
OF POOR QUALITY**

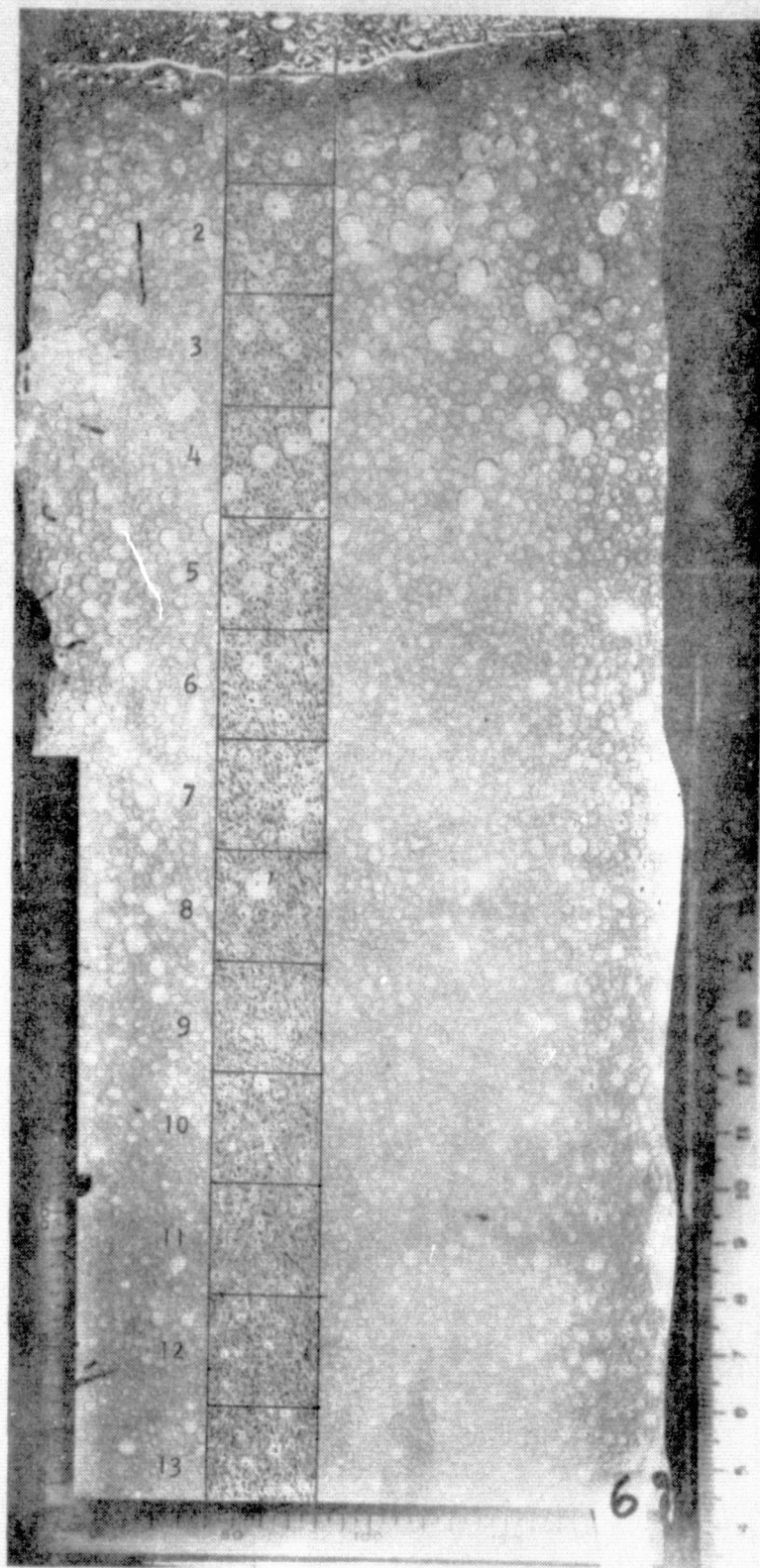


Figure 3-12 Enlarged Photo of Sea Water Foam, 70-100 Micrometer Glass Frit

**ORIGINAL PAGE IS  
OF POOR QUALITY**

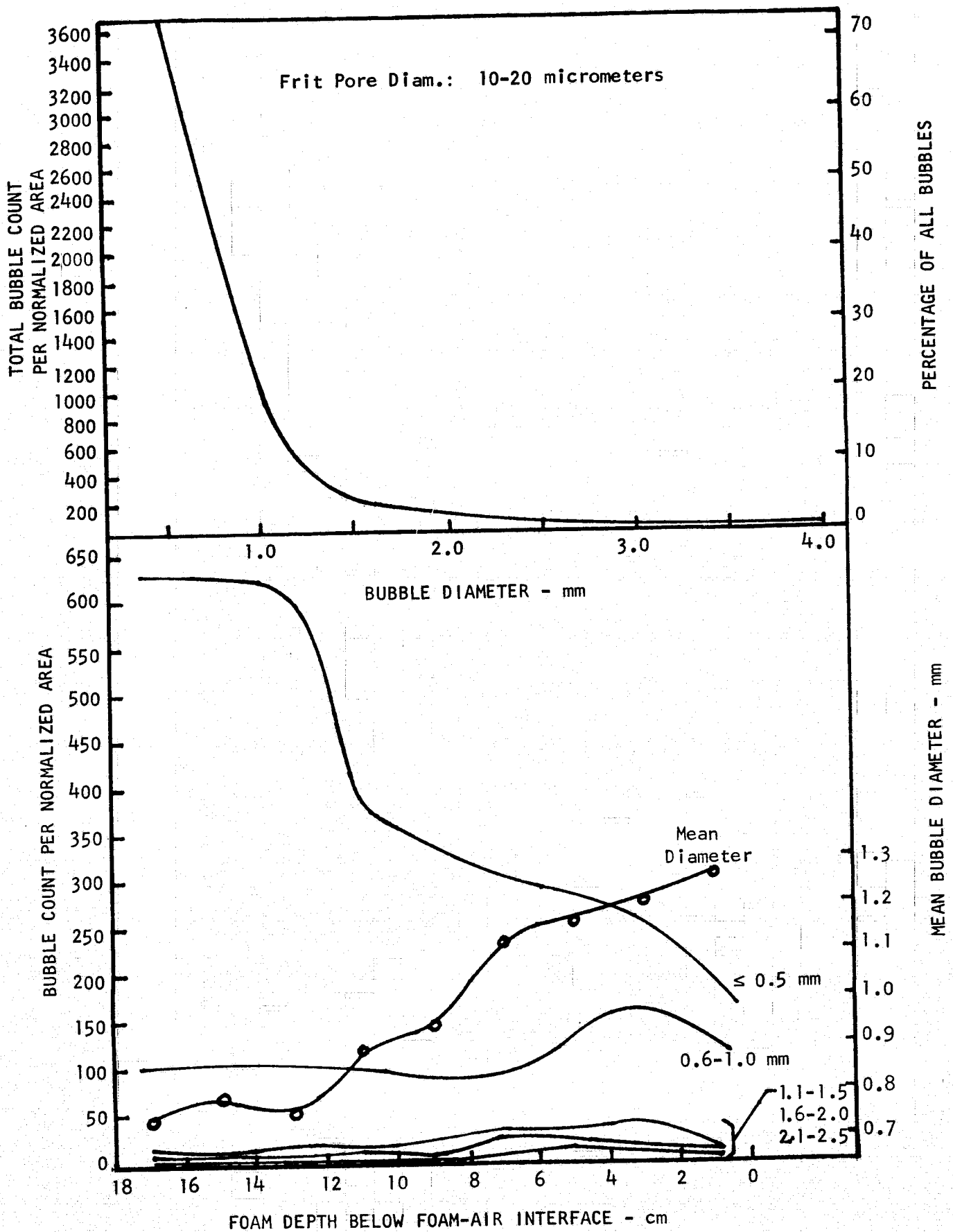


Figure 3-13 Foam Bubble Count as a Function of Bubble Diameter and Depth Below Surface

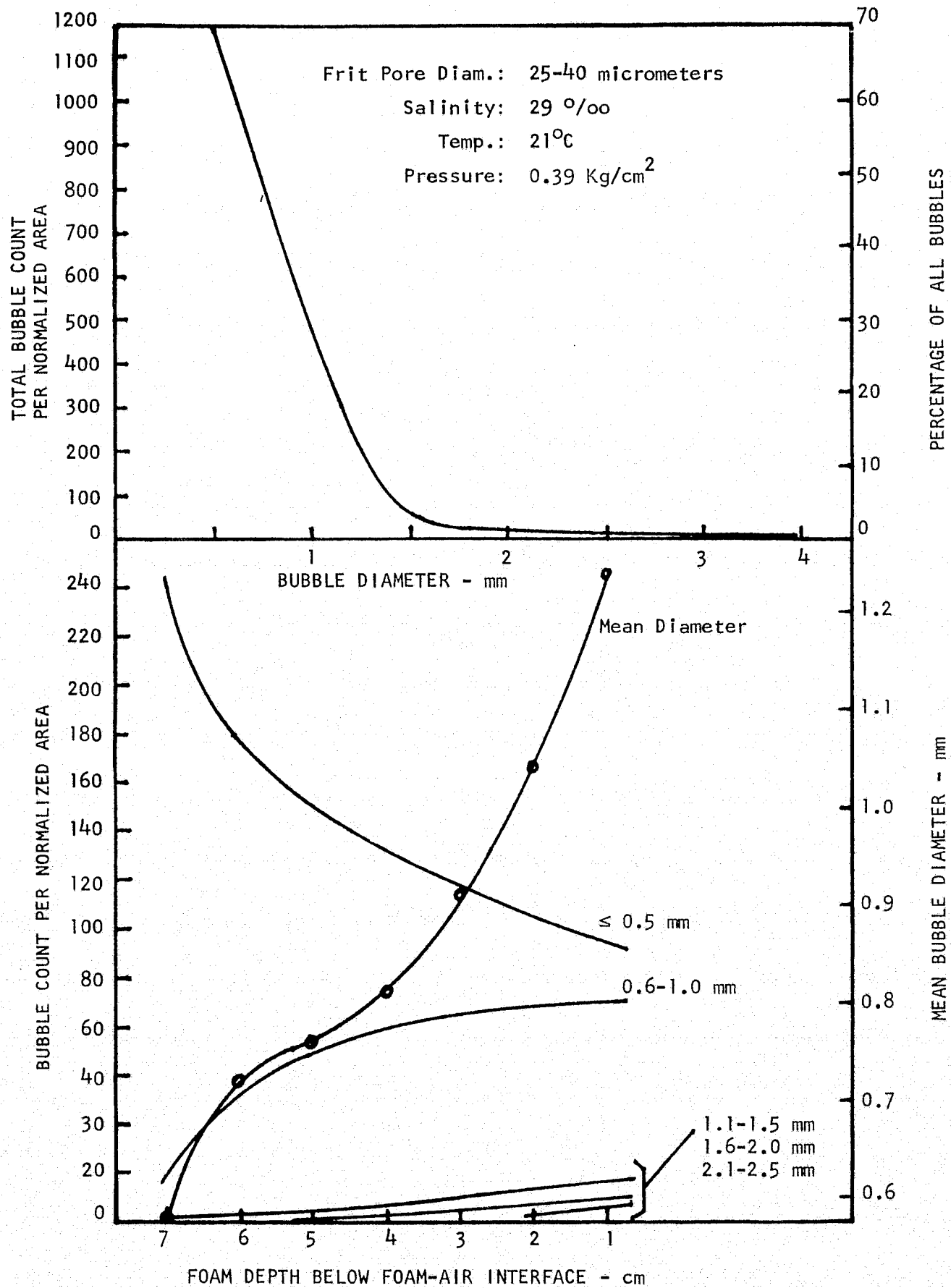


Figure 3-14 Foam Bubble Count as a Function of Bubble Diameter and Depth Below Surface

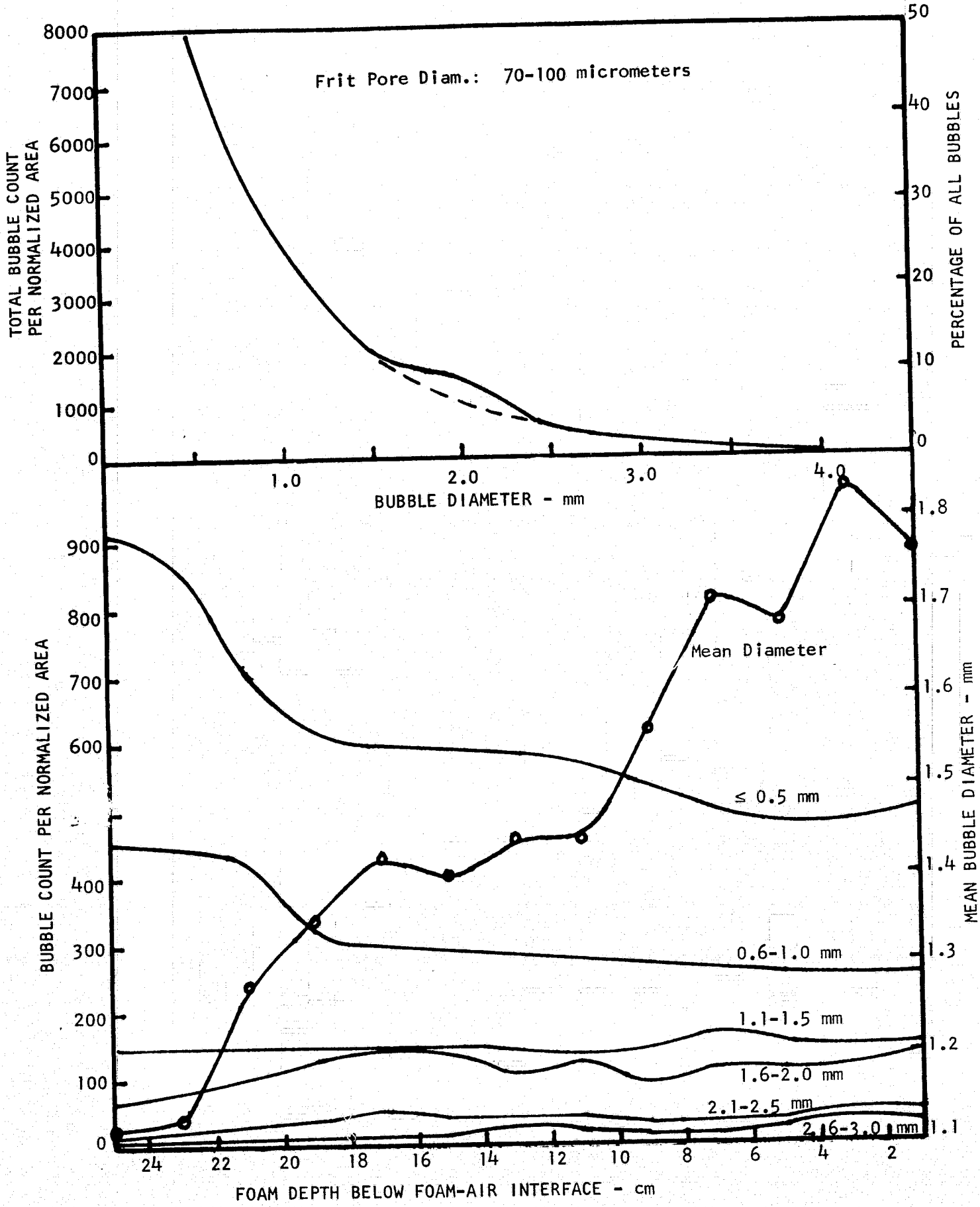


Figure 3-15 Foam Bubble Count as a Function of Bubble Diameter and Depth Below Surface



### 3.2.4 AIR AND WATER CONTENT OF OCEAN FOAM

The sampling procedure followed here was identical to that described in Section 3.1.4. The ocean water, used in this procedure, was described in Section 2.7.1. Sampling was carried out about one week after the ocean water was obtained; the water had been kept cool during this period, however, and showed a normal foaming ability. The water temperature at the beginning of this measurement was  $10.8^{\circ}\text{C}$ .

The water content of the foam, generated by the 25-40 micrometer frit, was very similar to that obtained with the first foam generator. It was noted that the water content of foam generated by the 10-20 micrometer frit was the most uniform at different depths, and at different foam heights; it was always in the range 25 to 35%. The top 4 cm of the foam, produced by the 70-100 micrometer frit had a water content of approximately 28%. For foam heights less than 7 cm, the water content of the top 4 cm rose linearly with decreasing foam depth to a maximum of about 45 to 50% at a depth of 4 cm. For reasons to be given in Section 3.4, the top 2-4 cm of foam, produced by the 70-100 micrometer frit, when the foam height is 10 cm or greater, appears to be most similar to much thinner foam occurring naturally on the ocean surface.

### 3.2.5 DIELECTRIC PERMITTIVITIES AND ELECTRICAL SKIN DEPTHS OF OCEAN FOAM

Dielectric permittivities and electrical skin depths were calculated for the three frequencies to be used at the NASA-Langley Research Center roof-top wave tank. The method followed was the same as presented in Section 3.1.5. The salinity was set at 33 ‰, and the water temperature at  $284^{\circ}\text{K}$ . These values are representative of those prevailing in the open ocean. Also, based on the air and water content studies, described in Section 3.2.4,  $V_w$  was set to 28%. This is considered to be close to the actual water content of ocean foam. The results of calculations, involving the electrical properties of ocean foam, at the three frequencies of interest in this study, are presented in Table 3-2. The notation is the same as that used in Section 3.1.5.

Table 3-2

## ELECTRICAL CHARACTERISTICS OF OCEAN FOAM

Frequency (GHz) →	1.43	2.65	7.29
$\lambda_o$ (cm)	20.98	11.32	4.15
$e_w^I$	74.18	72.17	45.37
$e_w^{II}$	57.71	40.39	39.86
$e_f^I$	21.49	20.93	14.26
$e_f^{II}$	16.16	11.31	11.16
$\tan \delta$	0.752	0.540	0.782
$\alpha \left( \frac{1}{\text{cm}} \right)$	0.492	0.663	3.399
$\frac{1}{\alpha}$ (cm)	2.033	1.508	0.293
DB loss/cm	4.27	5.76	26.92

The above results are representative of the anticipated electrical properties of ocean foam, for the given salinity and temperature. As would be expected, the Table shows that the skin depth of foam decreases drastically with increasing frequency.

### 3.3 RESULTS WITH THIRD FOAM GENERATOR

The third foam generator was constructed to investigate the foaming ability of a multi-frit array, since such a unit will be used in the NASA Langley Research Center wave tank. Three (3) 25-40 micrometer glass frits, mounted adjacent to each other, were operated all at once, and in pairs, to determine the amount of air required to generate specified foam heights. The fourth frit space, in the frit holder, was blanked off with a sheet of plexiglass, due to the lack of a fourth glass frit.

The frit in the corner opposite the plexiglass plate did not allow as much air flow as the remaining two frits, even though all were supposed to have the same

porosity. Even after adding an extra perforated copper tube, to permit a greater amount of air to be supplied to the defective frit, it still did not pass as much air as the other two frits. The pore diameters in this frit could have been much smaller than 25-40 micrometers.

The applied air flow was measured by a special flowmeter, furnished as GFE by NASA Langley Research Center. At an input air pressure of  $1.05 \text{ Kg/cm}^2$ , a steady air flow of 1.9 litres/sec., was read on the flowmeter. As expected, the greatest foam depth was obtained over the  $36 \times 36 \text{ cm}$  area when all three frits were uncovered. Under these conditions, the depth was 6.5 cm. It was observed that this maximum foam depth appeared to be somewhat insensitive to the initial amount of free-standing water in the tank before the application of pressurized air. Because of the limited capacity of the air compressor, and the range covered by the air flowmeter, pressures above  $1.05 \text{ Kg/cm}^2$  were not used. However, it is expected that a compressor supplying higher pressures and flow rates, working with a full frit array, with pore sizes in the 70-100 micrometer range, would produce considerably greater depths of foam.

#### 3.4 IN SITU OBSERVATIONS OF OCEAN FOAM

In order to determine which of the laboratory-generated foam samples most closely approximated the characteristics of ocean foam, it was desirable to examine the physical properties of ocean foam. A search was made for a suitable site at which photographs could be taken of foam generated by ocean breakers. A satisfactory location was found at a rocky promontory near the Lydia Pinkham mansion on Marblehead Neck, in Marblehead, Massachusetts. A meter stick with millimeter divisions was mounted on the end of a long wooden boom and extended close to the ocean surface. The meter stick was held in a manner that would allow it to lie near the surface of the foam produced by the wave action. To avoid spray from striking the camera lens, the camera was mounted on a tripod, at some distance from the water, and a 230-mm telephoto lens was used to photograph the meter stick during its immersions in foam.

Out of a total of 36 photographs, taken during the observations, only three (3) were found to have satisfactory information for further analysis. This was mainly due to the lack of sufficient foam at the time of the observations. The useful photographs were enlarged to  $20 \times 25 \text{ cm}$ . Areas of foam, with clearly-delineated bubbles, lying close to the millimeter scale on the meter stick, were marked off on

the photographs. The number of bubbles included within a certain bubble-diameter range were then tabulated. Bubbles with diameters greater than 2.5 mm were seen to comprise about 11% of the total number of surface bubbles in the foam, with the largest bubbles ranging in diameter up to 10 mm.

Figure 3-16 shows one of the in situ ocean foam photographs, with two marked foam areas lying close to the meter stick. These areas were used in the analysis of ocean foam bubble diameters.

ORIGINAL PAGE IS  
OF POOR QUALITY



Figure 3-16 Enlarged Photo of Natural Ocean Foam, with Meter Stick

## Section 4

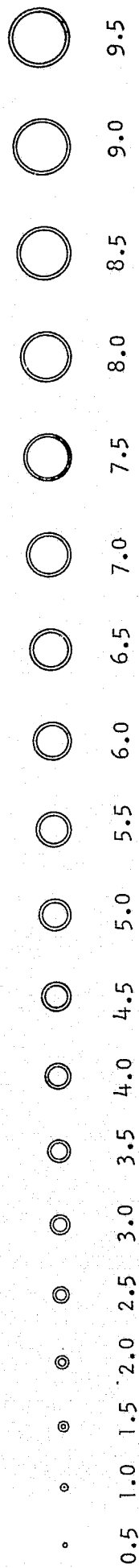
### TECHNIQUE FOR ROUTINE ANALYSIS OF OCEAN FOAM

#### 4.1 DESCRIPTION OF METHOD

In the early stages of this project, the analysis of the various foam photographs involved counting the number of bubbles of a certain size range as a function of depth in the foam. This was a tedious procedure, which often resulted in eye-strain. It consisted of the following steps:

- 1) The scales on an architect's ruler were examined to determine which one corresponded most closely with the millimeter scale appearing in the enlarged foam photograph;
- 2) The architect's scale was then used to measure the diameter of each bubble in each of the areas marked off on the 20 x 25 cm print;
- 3) As each bubble was measured and tabulated, it was marked off by pencil or pen, to avoid the possibility of accidentally counting it again.

The reflected glare of lights, and the very small size of the bubble images would often produce eye fatigue. To minimize this problem, and to expedite the entire procedure, an improved arrangement was devised. A 20 x 25 cm positive transparency was produced from the original Polaroid negative, in place of a print. This transparency was placed on a 25 x 25 cm light table. In a darkened room, the bubble images were quite distinct, and there was no reflected glare, since all the illumination was from behind the transparency. To provide a standardized counting scale which could be used to determine bubble size, regardless of the scale of the photograph under examination, a clear plastic template was produced, as shown in Figure 4-1. This consisted of a series of 19 circles, 17 of which were dual concentric circles. All the circle pairs, except for the two smallest, consist of an outer circle of diameter  $n \times 0.5$  mm, and an inner, concentric circle of diameter  $(n-1) \times 0.5$  mm. The outer diameters range from 0.5 mm to 9.5 mm. In measuring foam bubbles on the transparency, the template was moved over the selected bubble until



INSIDE DIAMETER OF OUTER CIRCLE - mm

Figure 4-1

Clear Plastic Template for Measurement of Foam Bubbles.

the bubble's perimeter was seen to lie completely within a given circle's annulus. The bubble was then included in the count of all bubbles associated in size with that particular circle. The bubble image was marked with a fine-tipped indelible-ink pen (Sanford's "Sharpie") to prevent it from being measured and counted again. After all the bubbles had been counted in this manner, the scaling factor between the diameters of the various circles on the template and the actual scale of the photograph was determined. This was done by comparing the diameters of the circles on the template with the millimeter scales in the foam photographs, and then assigning the appropriate diameter range to each of the circles and their associated bubble counts.

After performing actual bubble-counts with this method, it became clear that concentric circles were not needed to determine the diameter range of a given bubble image. A series of 19 single circles, beginning with a diameter of 0.5 mm and increasing in 0.5-mm steps, to a 9.5-mm-diameter circle, would suffice. When using this method, measuring and counting bubbles within a 2.5-cm-wide vertical column of foam is expected to take only about 5 minutes, for each 1-cm-high rectangular area.

#### 4.2 ANALYSIS OF SAMPLE PHOTOGRAPHIC SEGMENT

A foam photograph, taken with the first foam generator was selected for analysis by the above-described procedure. A vertical column 2.5 cm wide (in the scale of the photograph) was drawn on the transparency with a fine, black felt-tipped indelible marker. This was divided into 1-cm-high rectangular areas, as described in Section 3.1.1. The bubbles in each of these areas were measured and counted using the concentric-circle template. The sizes of the circles on the template were then compared with the millimeter scale on the photograph, to determine the actual diameter range for each circle pair.

The foam photograph used here had been previously analyzed by means of the original bubble measurement and counting method. However, the 2.5-cm-wide column of foam, chosen at that time, did not coincide, in horizontal position, with the 2.5-cm-wide column analyzed with the new method; there was an overlap of approximately 1 cm between the two columns. However, the bubble counts and resultant bubble size distributions, obtained with the new method, were essentially identical to the original results obtained with the much slower original method. The same relative numbers of small and large bubbles, as a function of depth in the foam,



were obtained as in the original counting and analysis. These results confirm the earlier statement that the vertical column delineating the foam area to be analyzed may be arbitrarily located at any position in the foam photograph.

## Section 5

### DISCUSSION OF RESULTS

One of the purposes of this study was to determine how closely laboratory-generated foam could be made to approximate the characteristics of natural ocean foam. Accordingly, the bubble counts of foam generated in the laboratory, using glass frits of porosities 10-20, 25-40 and 70-100 micrometers, were re-examined and compared with results obtained from photographic records of natural ocean foam.

Only the bubble counts for the top 2-4 centimeters of foam in each photo were considered, because it seemed unlikely that greater foam depths would have a significant effect on, or relationship with, surface bubble distributions. It was also recognized that foam is formed, basically, by forces acting on the surface of the ocean. In the case of wind-generated foam, the crests of waves tumble onto the surface below to create whitecaps. Also, when waves are dashed against a rocky shore, foam is generated as a result of collisions between the water and the rocks. It has been noted that the larger the force, the larger the quantity of foam, and the larger the typical bubble sizes produced. In the case of the foam generators, used in this project, the air forced through the fritted glass was the force acting against the water in the creation of foam. The amount of foam produced was proportional to the force applied with the air compressor.

This interpretation was confirmed by examining bubble counts in foam photographs showing widely differing depths (approximately 10 cm difference) produced by the same glass frit with different air pressures. Regardless of porosity used, the percentage of bubbles with diameters greater than 2.5 mm, chosen arbitrarily as the diameter separating "large" bubbles from "small" bubbles, in the top 4 cm of foam, increased by at least a factor of two (2) when the foam depth was increased from a low level (about 6 cm) to a high level (> 16 cm). However, in deep foam, the percentage of large bubbles, produced by the 70-100 micrometer frit was 7% — the number closest to that obtained with the natural ocean foam.

This implies that a large-scale foam-generating apparatus, simulating ocean foam characteristics, should use frits with pore diameters of at least 70-100 micrometers and should be capable of generating at least 10 cm of foam. It is important to note that only the top 2-4 cm of this artificially-generated foam, with depths  $\geq 10$  cm, would simulate the characteristics of the thin layers of foam ( $\leq 2$  cm thick) lying on the surface of the ocean.

The justification for choosing 28% as the approximate water content for ocean foam is now apparent. The calculated electrical skin depths presented in Table 3-2, for this water content value, are seen to range from approximately 2 cm, at 1.43 GHz, to somewhat smaller values at higher frequencies. If the foam depth is 10 cm, there will be at least 8 cm of foam beneath the top 2 cm. Thus, the laboratory-generated foam could be considered a semi-infinite medium at all three (3) frequencies listed in the above Table.

The temperature of the water, used in the foam generators, had very little effect on the amount of foam produced. The same foam depth was obtained, at a given air pressure and frit porosity, whether warm or cold ocean water was used in the foam generator. However, the water should not be more than a week old.

Although the length of time a given volume of foam took to dissipate was not measured during any of the experiments, it was noted that foam generated from colder water persisted for a longer period of time than foam generated from warmer water. However, provided a constant pressure and flow was maintained through the glass frit, the foam remained at a constant height indefinitely.

## Section 6

### FULL-SCALE FOAM GENERATOR

Toward the end of this project, a full-scale foam generator was designed for fabrication and use by the NASA Langley Research Center. This unit will be mounted in the NASA roof-top wave tank and will permit radiometric measurements of the apparent temperatures of ocean foam.

Since the results of this study showed that the 70-100 micrometer glass frit produced foam bubbles very similar to those found on the ocean, this pore size was selected for the frits to be used in the full-scale generator.

Based on the antenna beamwidths, associated with the NASA radiometers, the minimum diameter of the foam patch, to be produced by the generator, was specified at 1.2 meters (48 inches). Accordingly, the generator was designed with inside dimensions of 1.3 x 1.3 meters. Basically, the design consists of three (3) items, which are described in the following paragraphs.

1. A square outer watertight tank, consisting of an aluminum bottom and plexi-glass sides. The inside dimensions of this unit are 1.3 x 1.3 meters. The plexi-glass sides are 41 cm high.

2. An inner pan with a flanged upper surface, forming the foam generator, with provision for mounting an array of sixteen (16) glass frits on top of the pan. The frit dimensions are 30.5 x 30.5 cm (12 in. square) and the total area occupied by the frits is 1.2 x 1.2 meters. An airtight seal is provided, between the gridded frit mounting frame and the pan flange, by means of an "O" ring. An array of four parallel, perforated brass pipes, with inside diameters of 0.95 cm (3/8 in.) is located on the bottom of the pan. The pipes are joined at one end and brought out to the top of the outside tank, via a single pipe, for connection to an air compressor. The inner pan is filled with granulated charcoal, for uniform diffusion of air, supplied by the pipes, over the bottom surface of the glass frits.

3. A waterproof, portable box with plexiglass sides, to serve as a housing for photo floodlamps. This box is intended to be placed on top of the frit array, near one side of the tank, to provide backlighting for satisfactory foam photography. The box is 46 cm square and 61 cm high. A small, motor-driven fan is located on the bottom of the box, to provide air circulation. It is expected that the heat from the photo floodlamps could damage the front wall of the box, unless proper air circulation is maintained during lamp operation.

Considerable care must be exercised in sealing the glass frits into their supporting gridded frame. The frame was designed with an individual right-angle aluminum mounting space for each frit, fabricated from "tee" section aluminum. The outer perimeter of the frame has a right-angle cross-section. To provide a satisfactory air seal, filled epoxy must be applied to the horizontal and vertical surfaces of the frame. After the frits are put in place, additional sealing is accomplished, with filled epoxy, around the periphery of the assembly and along the joints between the frits and their tee-section frames. These joints are, then, covered with a flat-section gridded frame, which will adhere to the epoxy and, thus, provide a positive air seal at all joints between the frits and the mounting frame.

A positive air seal, around each frit and between the mounting frame and the inner pan, described in Paragraph 2, is important due to the fact that air leaks usually produce much larger foam bubbles than do the pores in the frits. A large number of such bubbles will seriously affect the bubble size distribution and alter the air-water ratio in the foam.

## Section 7

### CONCLUSIONS

Several important conclusions may be drawn from the results of this study. These are as follows:

1. Representative ocean foam may be generated in the laboratory using sea water in a glass frit foam generator, with frit pore diameters in the range 70-100 micrometers.
2. The maximum air pressure required with a single 70-100 micrometer glass frit, for a full head of foam, approximately 25 cm high, is of the order of  $0.1 \text{ Kg/cm}^2$  (approximately 1 psi).
3. To obtain the proper diameter foam bubbles on, and near, the surface it is necessary to produce a foam height of at least 10 cm in a glass frit generator.
4. The top 4 cm of foam, produced by a 70-100 micrometer glass frit generator, are most representative of the bubble sizes to be found in natural ocean foam.
5. With the 10-20 micrometer foam generator, 50% of all bubbles were  $\geq 0.75$  mm in diameter. In the top 4 cm of foam, the mean diameter ranged from 1.0 to 1.2 mm.

In the case of the 25-40 micrometer foam generator, 50% of the bubbles were  $\geq 0.72$  mm in diameter. In the top 4 cm, the mean diameter ranged from 0.94 to 1.22 mm.

Finally, in the case of the 70-100 micrometer foam generator, 50% of the bubbles were  $\geq 0.6$  mm in diameter. In the top 4 cm, the mean diameter ranged from 1.55 to 1.70 mm.

The maximum diameter of foam bubbles, measured during the course of this study, was 4 mm.

6. The water content of the top 4 cm of foam, produced by a 70-100 micrometer glass frit generator, is 28%, for total foam depths in excess of 7 cm.

7. The electrical characteristics of ocean foam may be determined by considering it to be a porous medium. On this basis, the ratio of the real part of the dielectric permittivity of ocean foam to that of ocean water, in the frequency range 1-10 GHz, is equal to 0.29. The ratio of the imaginary part of the dielectric permittivity of ocean foam to that of ocean water, in the same frequency range, is equal to 0.28.

8. The skin depth of ocean foam is 2.0 cm at 1.43 GHz, 1.5 cm at 2.65 GHz and 0.32 cm at 10.69 GHz. Thus, in this frequency range, ocean foam with a depth greater than 2 cm may be considered to be a semi-infinite medium. Accordingly, whitecaps may be treated as semi-infinite media, in computations of brightness temperatures of rough ocean surfaces. However, since foam streaks are only a few bubbles thick, it will be necessary to consider them and the underlying water as layered structures, over most of the above frequency range.

## Section 8

### RECOMMENDATIONS

The following recommendations are made as a result of this study:

1. The close physical relationship between bubbles produced by the 70-100 micrometer foam generator and those found in natural ocean foam suggests that glass frits, with pore diameters in the range of 70-100 micrometers, be employed in the full-size foam generator to be built by the NASA Langley Research Center.
2. The full-size foam generator should have a minimum foam area diameter of 1.3 meters.
3. For reasons of economy, the dimensions of the 70-100 micrometer glass frits should be no smaller than 30.5 x 30.5 cm.
4. All joints between the frits and their mounting frame should be thoroughly sealed with filled epoxy, to prevent air leaks past the frits.
5. Fresh sea water, free of pollutants, should be used in the generation of foam. Upon completion of a given experiment, the sea water should be pumped out of the foam generator, with the air compressor running, and the generator washed out with fresh water. To prevent any accumulation of fresh water in the charcoal bed under the frits, the compressor should be kept running during the washing process.
6. To obtain suitable bubble size distributions, a foam layer  $\geq 10$  cm deep should always be generated.
7. Polaroid positive-negative film, designated PN 105, should be used in the Model MP-4 camera for photographing foam. A 20 x 25 cm positive transparency should be produced from the film negative, for subsequent foam bubble analysis. The transparency may be conveniently examined on a light table.



9. The numerical procedures involved in producing plots of bubble size distribution and other data for laboratory-generated ocean foam are quite simple and straightforward. The calculations involved are not sufficiently complicated or laborious to warrant data processing on a large computer. It would take more time to set up the input data for a suitable reduction program than it would to perform the necessary computations on a pocket calculator such as an HP-35, HP-45, or TI SR-50. Some time saving could be achieved by performing the computations on a programmable calculator such as the HP-55 or HP-65.

10. Immediately after the full-size foam generator is placed into operation, the foam water content should be checked, at different depths in the foam, using a graduated beaker without a spout. A spout may allow the escape of foam bubbles, while enroute from some depth in the foam to the surface.

11. Following the determination of foam water content, its electrical characteristics should be checked, at frequencies of interest, using the procedures described in this report.

12. The brightness temperatures of rough ocean water should be calculated at frequencies of interest, using the improved COMTEMP program developed by this firm. This program includes a subroutine that brings in the contributions by whitecaps and foam streaks as a function of wind velocity.

13. The above brightness temperatures should be modified to bring in the effects of radiations received via the sidelobes of the antennas used in the NASA-Langley airborne radiometric systems. Useful comparisons could, then, be made between the modified brightness temperatures and apparent temperatures, obtained with the airborne system, over instrumented ocean areas. Any discrepancies between the theoretical and experimental data should be reconciled to the greatest degree possible. Favorable comparisons between theoretical and experimental data will permit highly useful theoretical predictions of the brightness temperatures of rough ocean surfaces, including whitecaps and foam streaks.

## Section 9

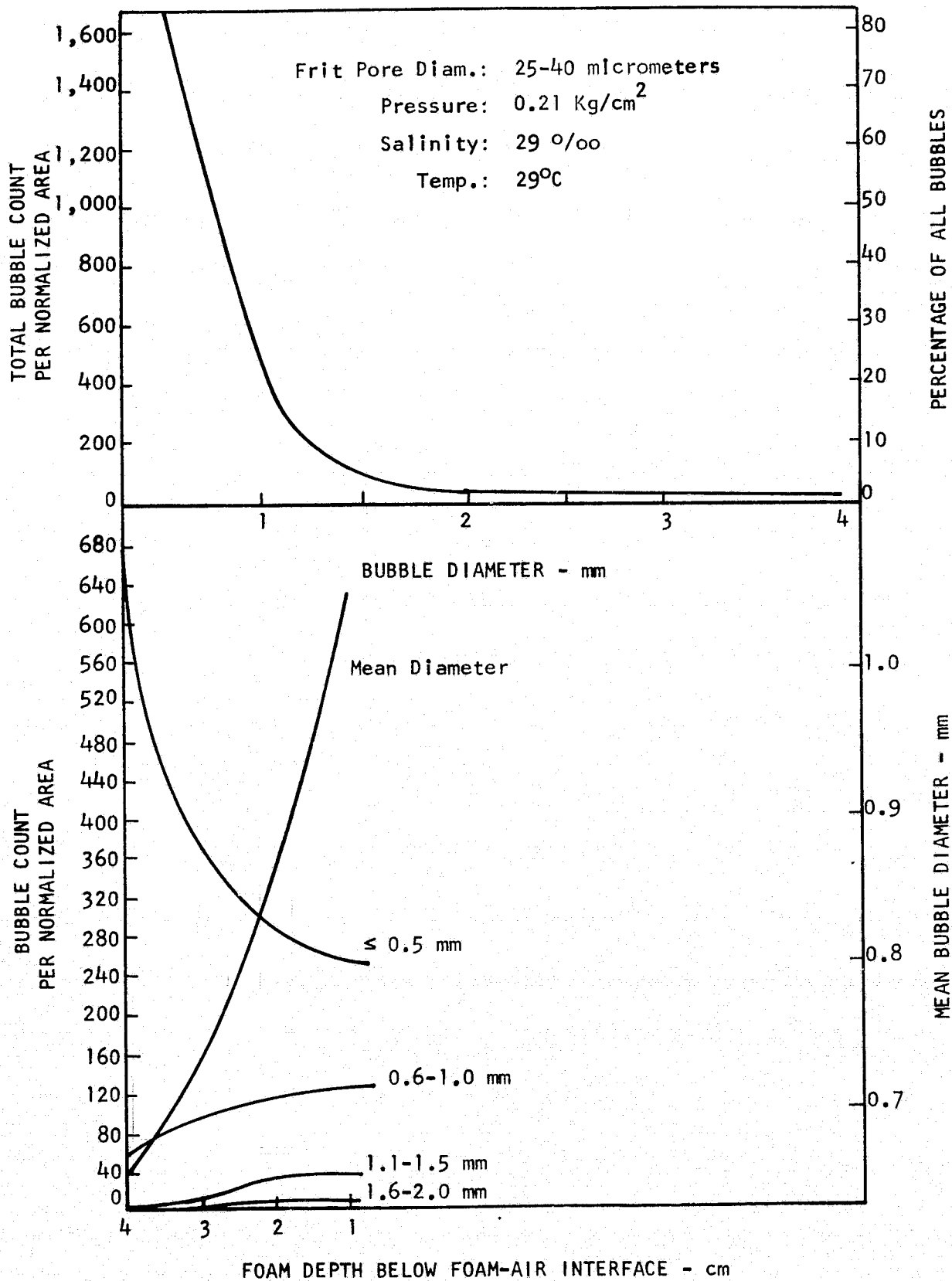
### REFERENCES

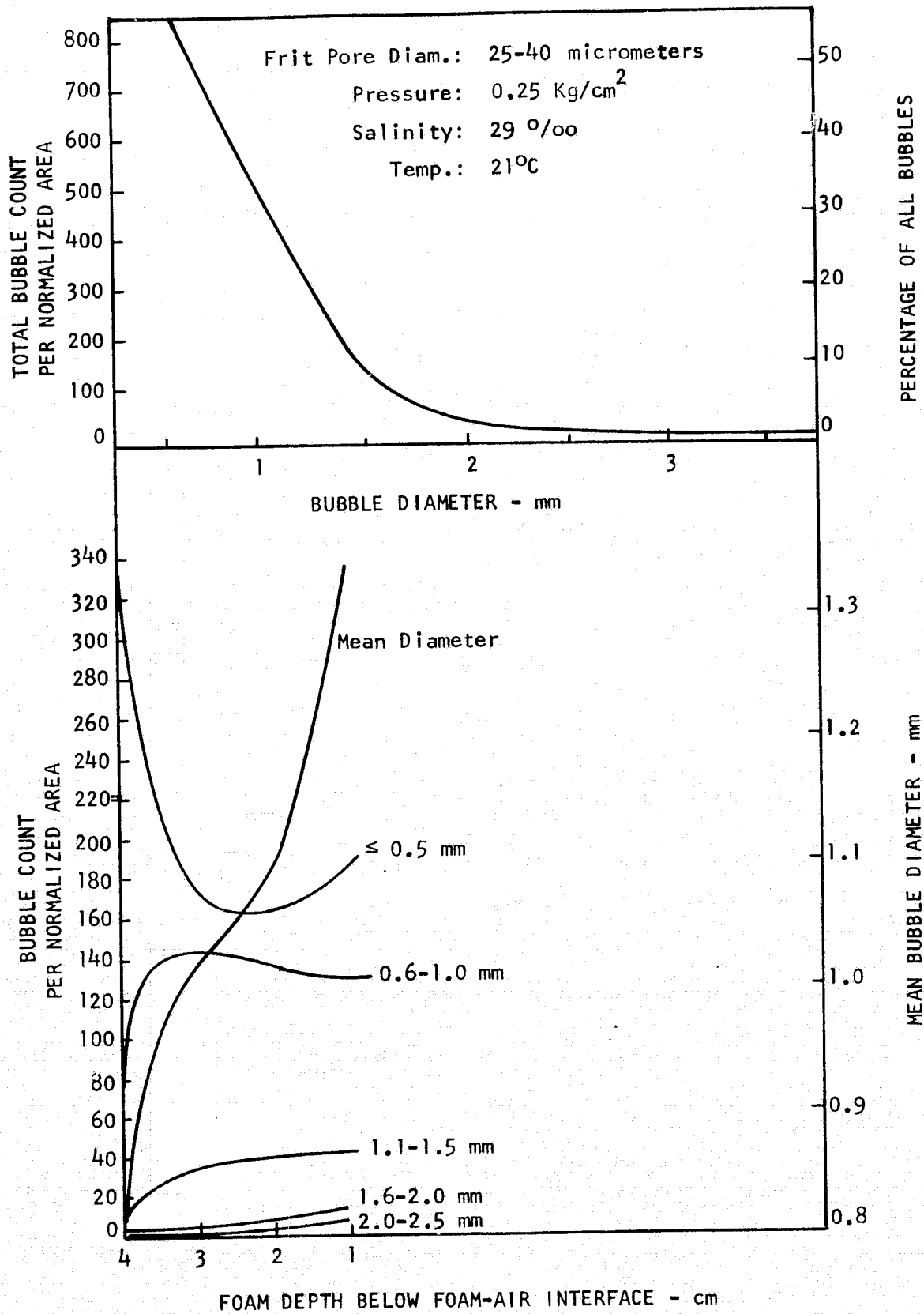
1. Hollinger, J.P., U.S. Naval Research Laboratory, Washington, DC — private communication.
2. Miyake, Y., and Abe, T., "A Study on the Foaming of Sea Water Part 1", *Journal of Marine Research* 7, 67, 1948.
3. Porter, R.A., and Wentz, F.J., III, "Microwave Radiometric Study of Ocean Surface Characteristics", NOAA Contract No. 1-35140, July 1971.
4. Von Hippel, A.R., "Dielectrics and Waves", M.I.T. Press, Cambridge, Mass., p. 28, 1954.

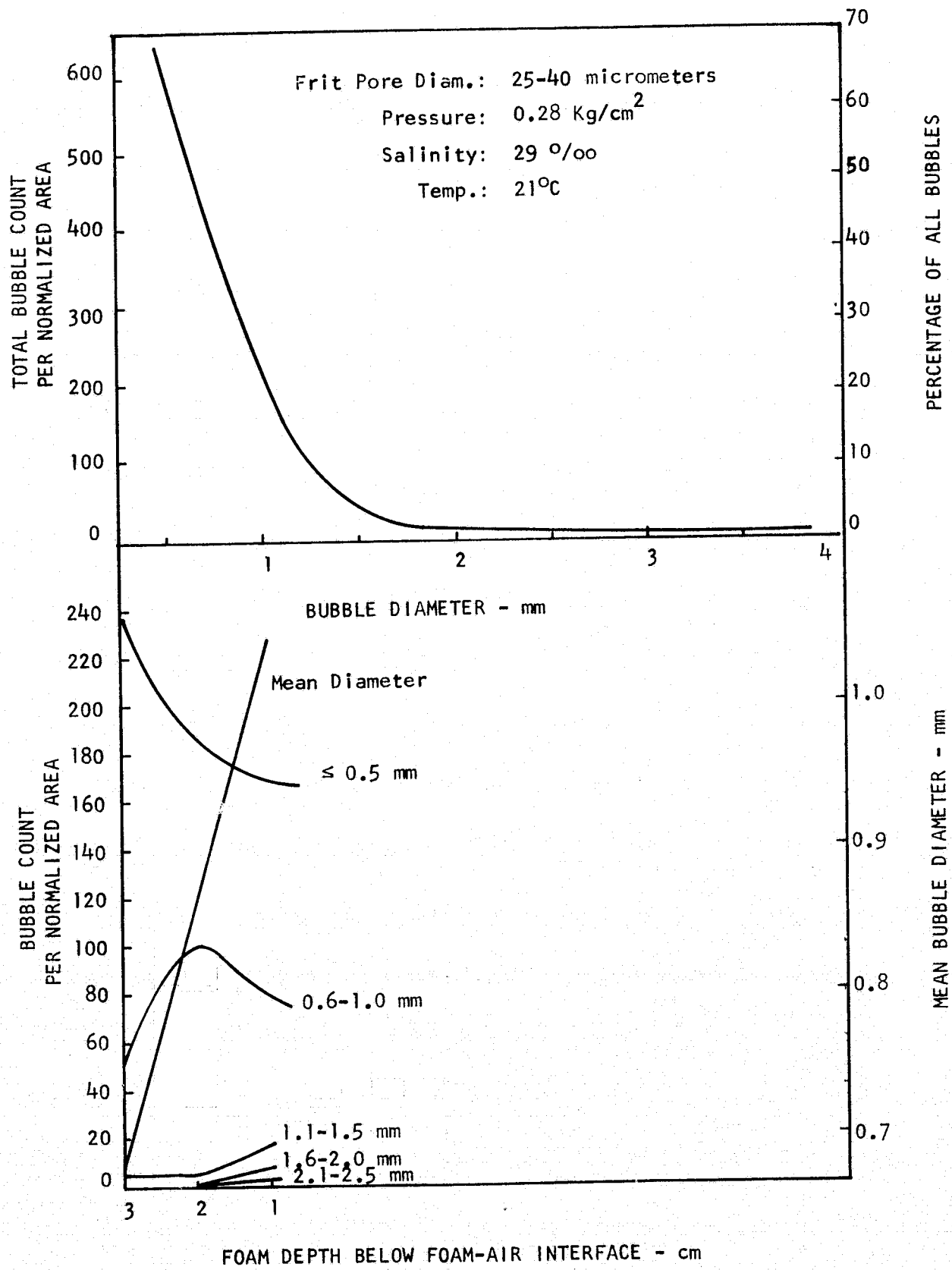
APPENDIX A

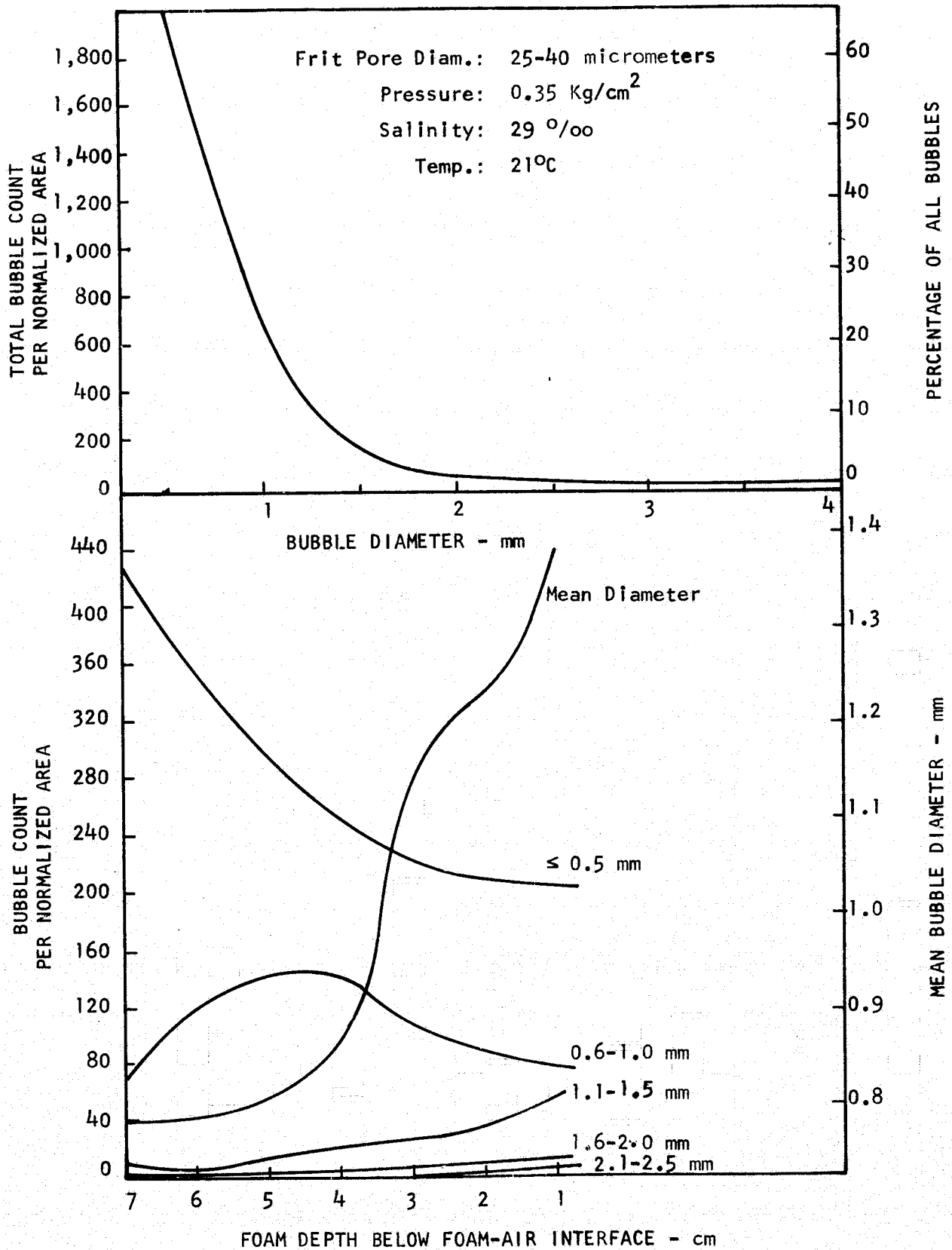
FOAM BUBBLE COUNTS OBTAINED  
WITH FIRST FOAM GENERATOR

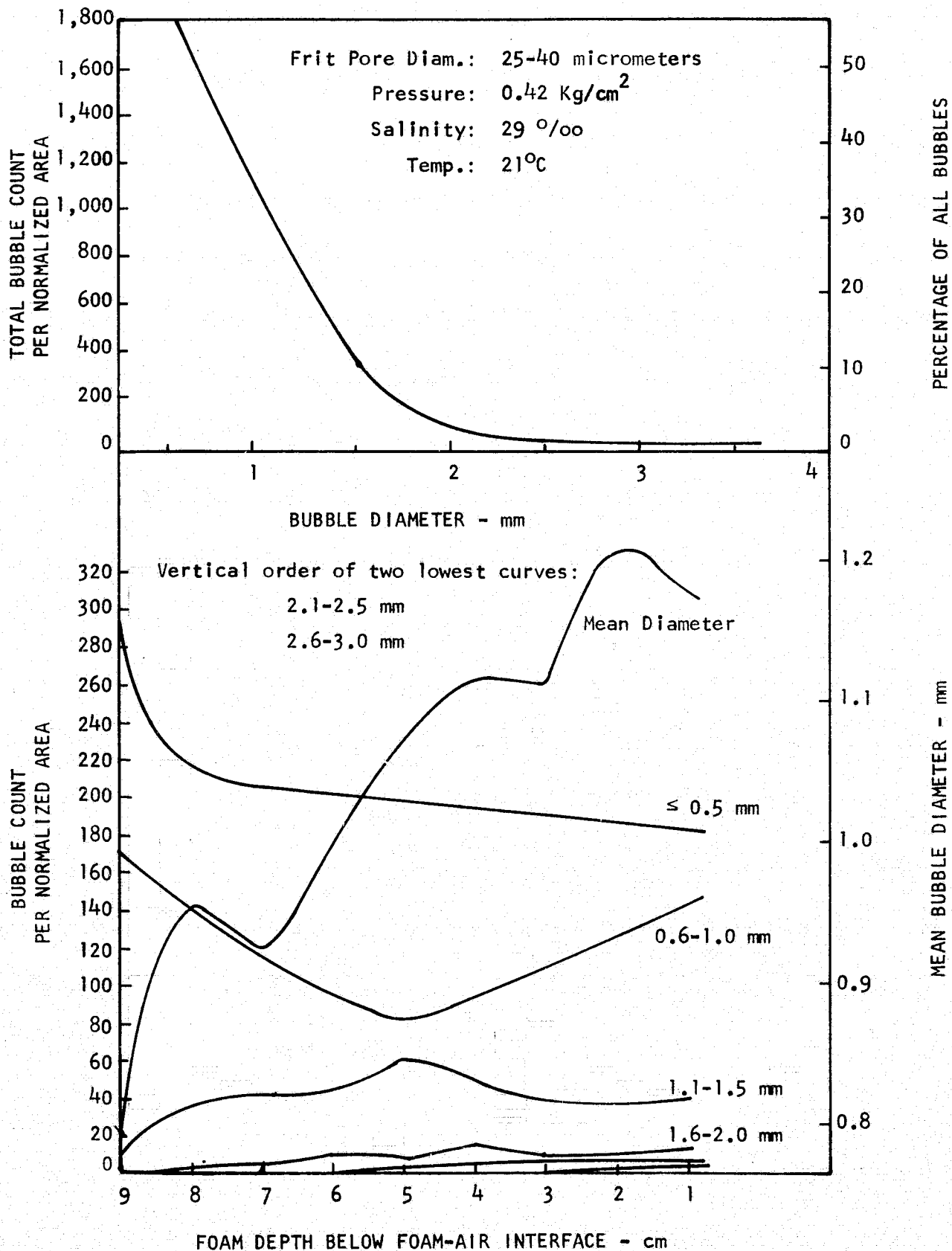
Frit Pore Diameter: .25-40 micrometers



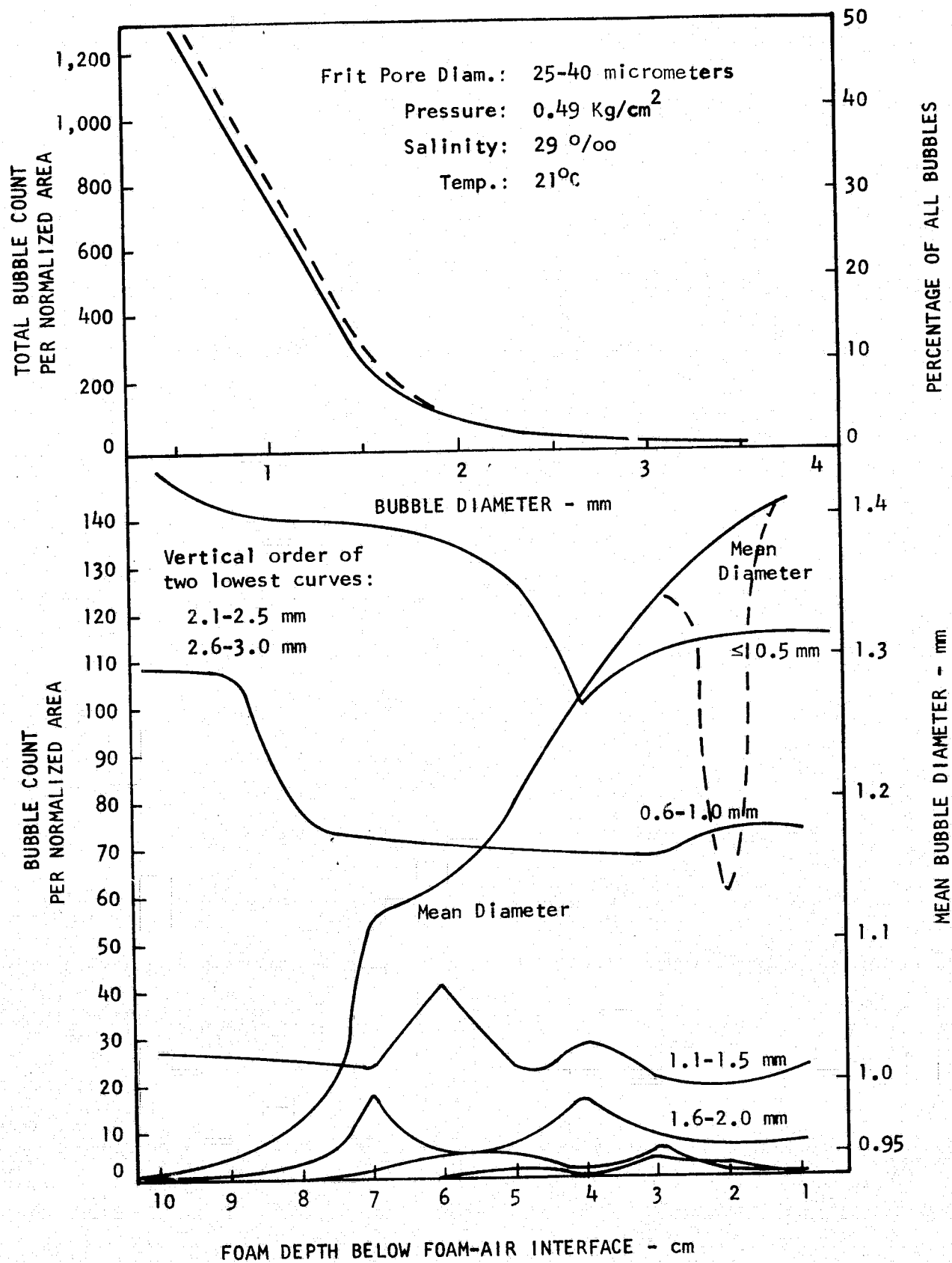


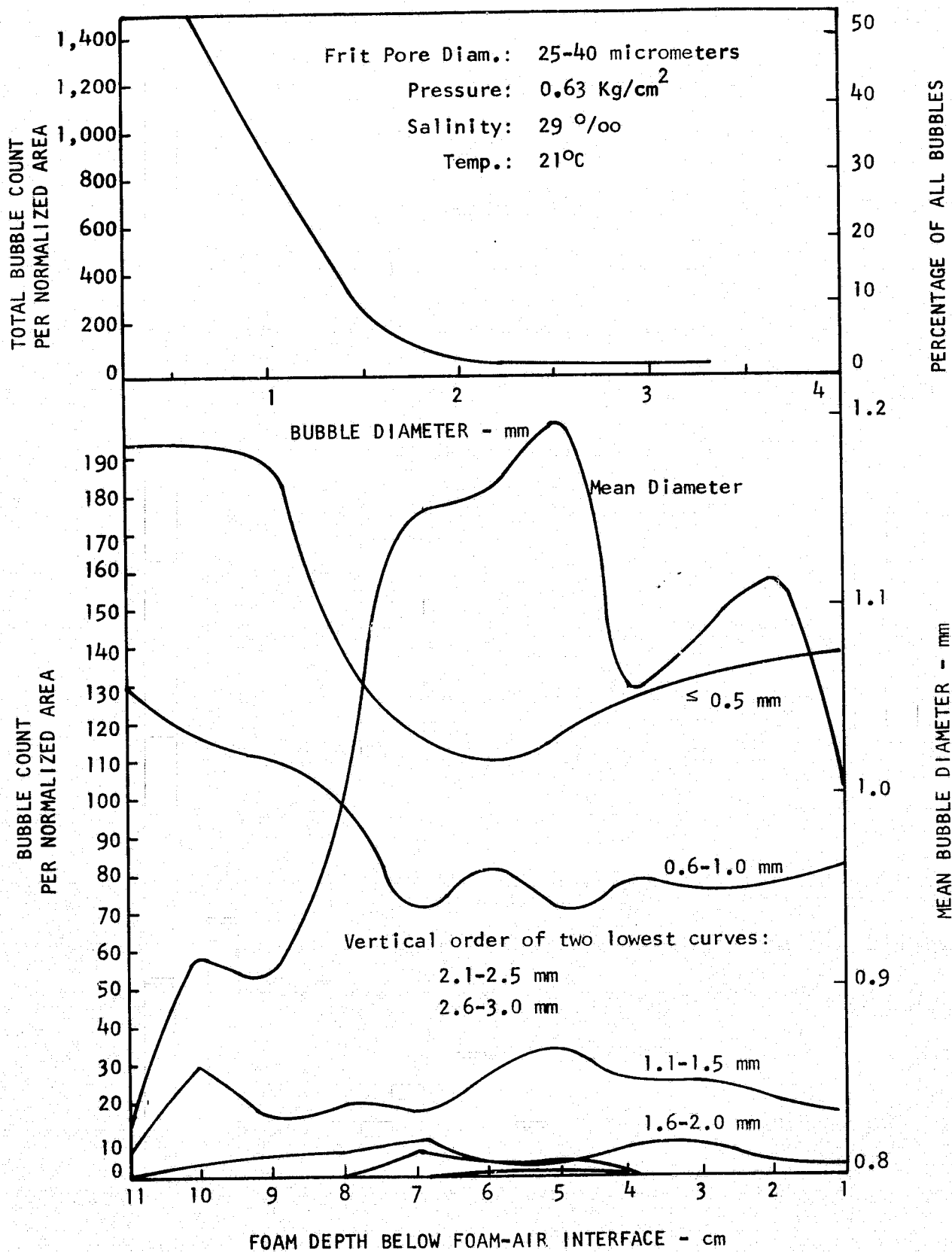












APPENDIX B

FOAM BUBBLE COUNTS OBTAINED

WITH SECOND FOAM GENERATOR

Frit Pore Diameters: 10-20 micrometers  
25-40 micrometers  
70-100 micrometers

